Extreme channelization of fluid and the problem of element mobility during Barrovian metamorphism

JAY J. AGUE[1,2,*]

[1]Department of Geology and Geophysics, Yale University, P.O. Box 208109, New Haven, Connecticut 06520-8109, U.S.A.
[2]Peabody Museum of Natural History, Yale University, New Haven, Connecticut 06511, U.S.A.

ABSTRACT

Geochemical profiles across chemically altered zones (selvages) surrounding amphibolite facies quartz+kyanite veins were investigated to determine major, minor, and trace element mass transfer and volume strain due to channelized fluid flow. The three profiles are perpendicular to two veins cutting the Wepawaug Schist, Connecticut, U.S.A., which underwent Barrovian-style metamorphism during the Acadian orogeny. Selvages are highly aluminous with considerably more kyanite, staurolite, and garnet, and less quartz, plagioclase, and mica, than surrounding wallrocks. Kyanite crystals increase in size toward veins, and reach several centimeters in length within veins. Mass balance analysis indicates 50% silica loss and 34% volume loss from selvages, on average. Silica, transferred locally from selvages to veins, accounts for 40 to 80% of the vein silica; the remainder must have been precipitated from fluids that flowed through the veins during regional devolatilization. Fluid flow also transported elements into the rock mass, which were concentrated in the selvages. Gains of Fe, Mn, Y, and HREE were due to the growth of selvage garnet; Fe, Zn, and Li were sequestered into staurolite. Kyanite, staurolite, and garnet growth resulted in Al mass gains. Destruction of mica (particularly muscovite) and of plagioclase in the selvages resulted in losses of K, Na, Ba, Pb, Sn, and volatiles and losses of Na, Sr, and Eu, respectively. Thin Na and Sr enrichment zones associated with increased modal plagioclase are found along the margins between selvages and less altered wallrock and may represent either chemical self-organization produced during diffusive mass transfer and reaction, or are relics from a possible earlier period of Na enrichment in the selvages.

Simple, two-dimensional numerical modeling of flow in a fractured porous medium indicates that fluxes vary significantly over short distances (<1 m) adjacent to veins. Fluids, channelized into the high-permeability fracture conduits, carry the bulk of the fluid flow; mass transfer to and from selvages adjacent to the conduits occurred by some combination of diffusion and flow. In contrast, areas distal to the conduits are impoverished in fluid and undergo much more limited infiltration. As a consequence, different workers can come to vastly different conclusions about the magnitude of fluid fluxes and element transfer depending on the part of a fractured outcrop studied. This extreme spatial variability due to channelization can largely explain contrasting views that have arisen in the literature regarding the nature and intensity of non-volatile element mass transfer during Barrovian metamorphism. Determining "average" time-integrated fluid fluxes and levels of element transport across outcrops remains as important research challenges due to the spatial variability of flow.

Keywords: Fluid flow, metamorphism, Barrovian, veins, element mobility, modeling

INTRODUCTION

Large fluid fluxes can transport mass and heat during metamorphism. For example, the impact of metamorphic volatiles on subduction zone processes including mantle metasomatism and arc magma genesis is widely acknowledged (e.g., Bebout and Barton 1989; Sorensen and Grossman 1989; Manning 1997; Spandler et al. 2004; Miller et al. 2009; Beinlich et al. 2010). There is also no doubt that fluid flow and element transport can control reaction progress in many other metamorphic environments, including shear zones (e.g., Dipple et al. 1990; Selverstone et al. 1991; Dipple and Ferry 1992) and contact and regional metamorphism of metacarbonate rocks (e.g., Orville 1969;

Hewitt 1973; Brady 1977; Tracy et al. 1983; Ague 2003a; Durand et al. 2009). Considerable disagreement persists, however, regarding the role of volatiles in collisional Barrovian settings. In fact, despite decades of study, the problem of whether or not large-scale fluid flow and mass transfer are integral parts of regional metamorphism remains controversial (cf. Evans 2007; Yardley 2009). Some workers have concluded that metapelitic rocks can undergo significant compositional changes as a result of metamorphic fluid infiltration (e.g., Ague 1994a, 1994b; Oliver et al. 1998; Masters and Ague 2005), whereas others argue that such changes are rare (e.g., Yardley 2009), minor, or non-existent (e.g., Shaw 1956; Walther and Holdaway 1995; Moss et al. 1996).

Yardley (2009) argues against "widespread and pervasive large fluid fluxes" during regional metamorphism because fluid

---

flow is largely upward and, therefore, regional-scale recirculation of fluid is unlikely. Nonetheless, quantitative numerical models show that large time-integrated fluid fluxes of $\sim 10^3$ $m^3_{(Fluid)}\ m^{-2}_{(Rock)}$ can be achieved during regional metamorphism of pelitic rocks in collisional orogens (Lyubetskaya and Ague 2009), even in the absence of convective circulation. Despite these large predicted fluxes, however, rocks that have undergone little discernable fluid infiltration are commonly encountered in outcrop-scale studies.

This apparent discrepancy could be explained if fluid flow was highly channelized into conduits such as permeable layers, shear zones, or fractures, leaving the rest of the rock mass relatively impoverished in fluid. Indeed, channelization of metamorphic fluids is widely inferred based on field, petrologic, and geochemical data (Rye et al. 1976; Ferry 1987; Bebout and Barton 1989; Selverstone et al. 1991; Dipple and Ferry 1992; Oliver 1996; Harlov et al. 1998; Oliver et al. 1998; Beinlich et al. 2010). In particular, quartz veins are mineralized fractures that can channelize large fluid fluxes. Chemical and isotopic metasomatism in alteration halos (selvages) adjacent to vein conduits has been documented for many years in the economic geology literature (e.g., Meyer 1965; Brimhall 1977, and references therein). A growing body of evidence indicates that veining and selvage formation can also be important during regional metamorphic fluid flow through aluminous metapelites (Ague 1994b; Oliver et al. 1998; Masters and Ague 2005; Penniston-Dorland and Ferry 2008; Beitter et al. 2008; Bucholz and Ague 2010). However, much remains to be learned, as the scale of alteration can vary considerably between studies, as can the time-integrated fluid fluxes and the suites of mobile elements. A further complication is that some veins may form mostly by local "segregation" or "differentiation" processes involving little fluid flow, whereas others may be conduits for substantial fluid volumes (cf. Yardley 1975; McLellan 1989). These different styles of veining can be present in the same outcrop, particularly when multiple vein generations developed at different times under different conditions in the metamorphic cycle.

Barrovian terranes make up the bulk of the exposed metamorphic rocks in mountain belts worldwide. Consequently, it is critical to determine if this type of metamorphism generates large-scale fluid fluxes that are ultimately important in the global cycling of elements. To address this and related issues, I focus on quartz-kyanite veins of the Wepawaug Schist, Connecticut, a well-studied rock unit that underwent Barrovian-style metamorphism during the Acadian Orogeny. A mass balance analysis is presented that quantifies chemical changes associated with veining, together with simple two-dimensional (2D) modeling of fluid flow that places constraints on the degree of channelization that can be attained in fractured outcrops. The ultimate goals are to determine if strongly channelized, syn-metamorphic fluxes: (1) were large enough to transport elements into and out of the rocks and (2) can help to explain strongly contrasting views regarding the amount and nature of fluid flow in Barrovian terranes.

GEOLOGIC SETTING AND PREVIOUS WORK

The Wepawaug Schist consists predominantly of metapelitic rocks, but also contains lesser amounts of metacarbonate, metapsammite, and felsic igneous and metaigneous rocks (Fritts 1962,

1963, 1965a, 1965b; Hewitt 1973; Tracy et al. 1983; Palin 1992; Ague 1994a, 1994b, 2003a). Metamorphic grade increases from the chlorite zone in the east, through a biotite-garnet zone, and finally to the highest-grade staurolite-kyanite zone rocks in the west (Fig. 1). Metamorphic temperatures (T) and pressures (P) increase from $\sim$420–430 °C and $\sim$0.6–0.7 GPa in the east to $\sim$610–620 °C and $\sim$0.8–1.0 GPa in the west (Ague 2003a). The rocks were deformed and metamorphosed as a result of the collision of Avalonia with ancient eastern North America during the Devonian Acadian orogeny (cf. Hibbard et al. 2007). Metamorphic heating was concentrated into two pulses, one $\sim$389 Ma and the other, corresponding to peak thermal conditions, at $\sim$380 Ma (Lancaster et al. 2008).

Quartz veins are widespread in the Wepawaug Schist, and increase in abundance from several volume percents in the
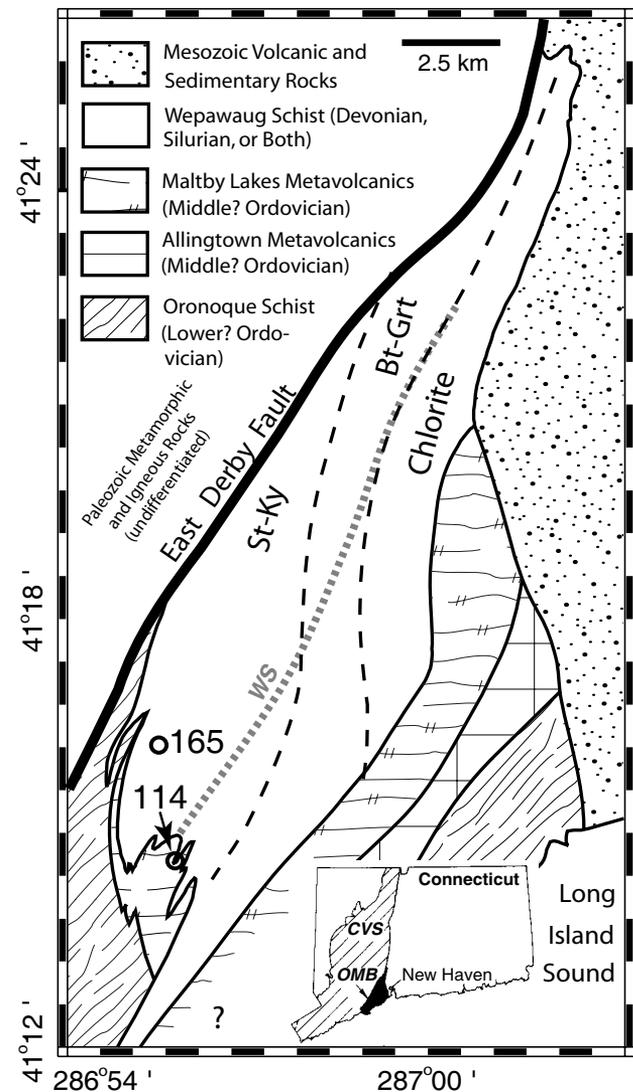
FIGURE 1. Geologic sketch map of the Wepawaug Schist, part of the Orange-Milford belt (OMB) of the Connecticut Valley Synclinorium (CVS). Sample localities JAW114 and JAW165 shown with open circles (prefix JAW omitted for clarity). WS = Axis of Wepawaug syncline. Modified after Fritts (1963, 1965a, 1965b) and Rodgers (1985). Isograd positions after Ague (2003a).
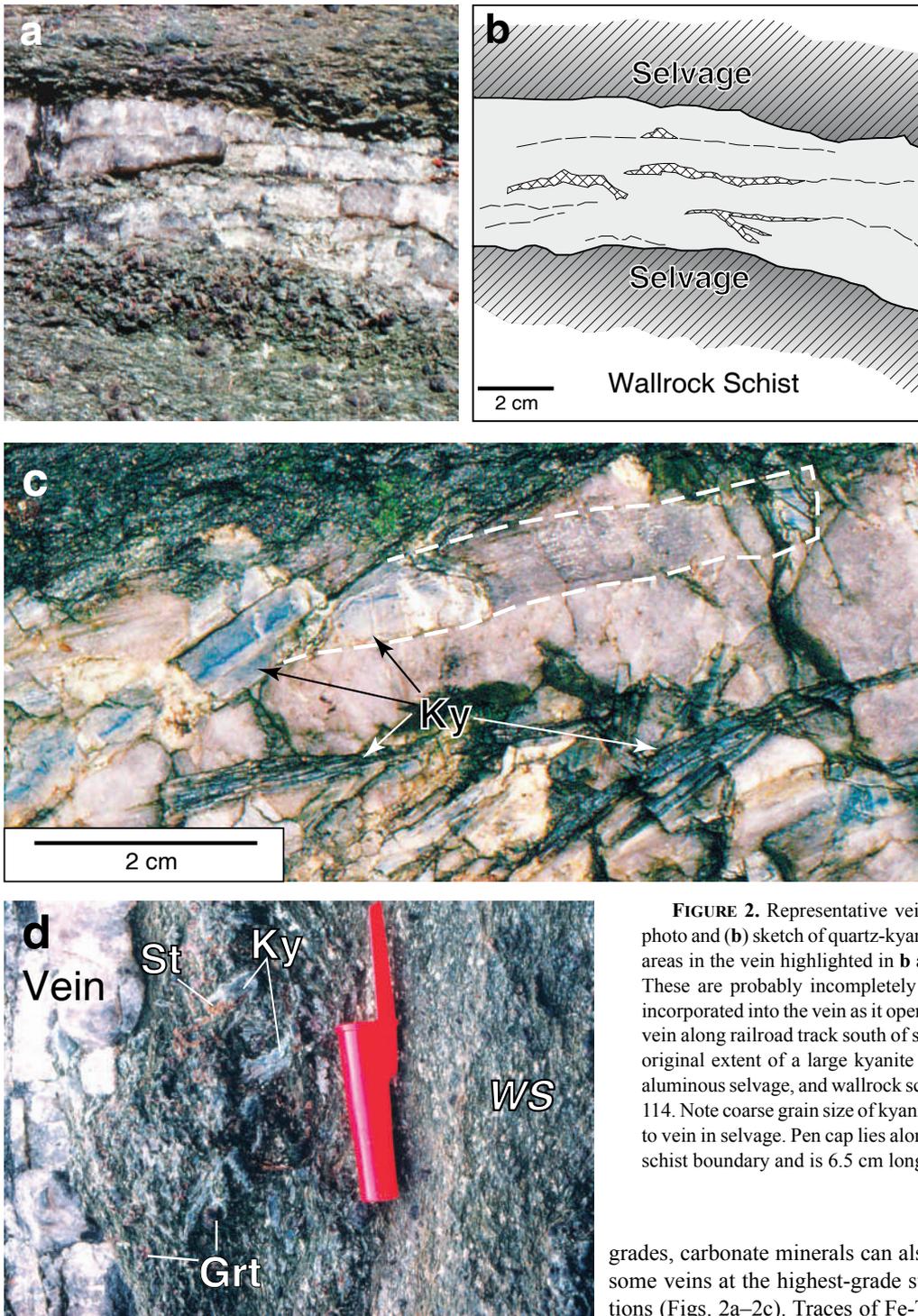
FIGURE 2. Representative vein-selvage relations. (**a**) Outcrop photo and (**b**) sketch of quartz-kyanite vein at site 114. Crosshatched areas in the vein highlighted in **b** are areas rich in kyanite crystals. These are probably incompletely digested fragments of wallrock incorporated into the vein as it opened. (**c**) Kyanite crystals in quartz vein along railroad track south of site 165. White dashed line shows original extent of a large kyanite crystal. (**d**) Quartz vein (at left) aluminous selvage, and wallrock schist beyond selvage margins, site 114. Note coarse grain size of kyanite, garnet, and staurolite adjacent to vein in selvage. Pen cap lies along approximate selvage-wallrock schist boundary and is 6.5 cm long. *WS* denotes wallrock schist.

chlorite zone to 20–30% in the staurolite-kyanite zone (Ague 1994b). They were among the first, if not the first, metamorphic veins described in a North American scientific publication. Silliman (1820) described the rock as "…abounding with veins and distinct tuberculous masses of quartz occasionally of enormous size…" Quartz is overwhelmingly dominant in most veins (Fig. 2). Plagioclase is the most common accessory mineral in veins that contain additional phases; micas, sulfides and, at the lowest

grades, carbonate minerals can also be found. Kyanite grew in some veins at the highest-grade staurolite-kyanite zone conditions (Figs. 2a–2c). Traces of Fe-Ti oxides have been found in a few veins cutting upper greenschist and amphibolite facies rocks. Veins at all metamorphic grades contain inclusions of wallrock that were dislodged from vein-wallrock contacts during vein opening.

Earlier studies concluded that fluid flow through fractures drove metasomatic reactions that resulted in significant chemical changes in alteration selvages adjacent to veins (Ague 1994b; van Haren et al. 1996). These included local losses of silica to veins and, at scales larger than local vein-wallrock systems, gains of Zn and Mn as well as mass transfer of alkali and alka-

line earth metals (Ague 1994b, p. 1105). The general process likely had three main facets. (1) Fracturing, which produced high-permeability conduits for flow. (2) Fluid flow through the fractures deposited quartz as part of the regional flow regime. Metasomatic interactions between these fluids and adjacent vein margins (selvages) produced chemical, mineralogical, and isotopic alteration. Ague (1994b) concluded that this alteration, particularly the loss of alkalis, led to the stabilization and growth of staurolite and kyanite in the most heavily altered vein selvages. Core-to-rim $\delta^{18}O$ increases of ~2 per mille in selvage garnet were interpreted by van Haren et al. (1996) to record the passage of large volumes of ascending, cooling fluids. (3) Diffusion of silica from selvages to fractures, which sealed them. On average, roughly 70% of the silica was derived locally, and 30% was precipitated by through-going fluids. The above "crack-flow-seal" process was probably repeated many times to build up typical veins (Ramsay 1980; Ague 2003b), as evidenced by observed textural relations (Ague 1994b).

The conclusion that metamorphic fluid flow could drive significant chemical changes in common types of metapelitic rocks beyond simple volatile loss was controversial (Ague 1995, 1997; Walther and Holdaway 1995; Moss et al. 1995), and even now remains a subject of vigorous debate (e.g., Evans 2007; Yardley 2009). Ague (1994b) did not measure detailed chemical profiles adjacent to veins; instead, a total of six samples taken at varying distances from veins in two outcrops were studied via mass balance and reaction progress approaches. In an effort to address the problem of metasomatism from a fresh perspective, the new work discussed herein presents high spatial resolution chemical data for 27 samples collected along three traverses perpendicular to two different quartz-kyanite veins. The large number of samples

allows rigorous statistical analysis of mass changes. Importantly, these veins are different from those studied by Ague (1994b) or van Haren et al. (1996), facilitating a comparison of results.

SAMPLES AND ANALYTICAL METHODS

The two sample localities are shown on Figure 1. Sites JAW114 and JAW165 contain ~31% and ~26% veins by volume, respectively (Ague 1994b). The site 114 vein is 4.25 cm wide, and is bordered on either side by highly aluminous, kyanite-rich selvages that are ~4 cm wide (Figs. 2a, 2b, and 2d). The selvages are rich in garnet, kyanite, and biotite, and are relatively poor in quartz, plagioclase, and muscovite (Figs. 2d and 3b). Staurolite is present in some samples. Rutile, in some cases rimmed by ilmenite, is a common accessory mineral. Beyond the selvage margins, quartz, plagioclase, and muscovite become more abundant, garnet is less abundant, and kyanite and staurolite are rare or absent (Figs. 2d and 3c). Pre-existing mica-rich fabrics are essentially obliterated in the selvages (compare Figs. 3b and 3c). The vein is composed almost entirely of quartz, but also contains accessory kyanite and rare traces of rutile (Fig. 3a). A profile, consisting of six samples (114i–114vi), was done on one side of the vein perpendicular to the vein-selvage contact. In addition, one selvage sample in contact with the vein was taken from the other side (114o).

Site 165 is a large (~1 m³) boulder blasted from an adjacent outcrop during railroad construction. The vein is 40 cm wide at its widest point; aluminous selvages on either side are ~16–18 cm wide. Selvages are composed mostly of garnet, kyanite, staurolite, biotite, and muscovite, but also contain lesser amounts of quartz and plagioclase (Fig. 3e). Accessory Fe-Ti oxides, organic matter, and sulfides are widespread. As is the case for site 114, less altered wallrocks beyond the selvage margins contain considerably more quartz, plagioclase, and muscovite, less garnet, and little or no kyanite and staurolite; selvage formation destroyed earlier micaceous foliations (compare Figs. 3e and 3f). The vein consists mostly of quartz±kyanite, but one area contains a mass of intergrown quartz, plagioclase, kyanite, and minor staurolite and biotite roughly 30 cm long and a few centimeters wide (Fig. 3d). Traces of rutile or ilmenite are occasionally found. Two traverses were done perpendicular to vein-wallrock contacts, one on each side of the vein. The south (S) profile is 26 cm long and consists of 10 samples, and the north (N) profile is 49 cm long and consists of 11 samples.

The identification of the boundary between the selvages and the less altered

TABLE 1. Major, minor, and selected trace elements

	x (cm)	Type	SiO₂	TiO₂	Al₂O₃	Cr₂O₃	Fe₂O₃	MgO	MnO	CaO	Na₂O	K₂O	P₂O₅	LOI	Total	Rb	Sr	Ba	Y	Zr	Nb	wRE
Site 165 South
165B	2.0	S	40.5	1.54	34.0	0.03	11.54	2.98	0.45	1.83	0.90	2.30	0.32	2.65	99.23	179	77	284	57	445	37	0.1149
165C	12.0	S	38.3	1.89	29.7	0.03	13.06	5.13	0.30	1.04	0.87	4.67	0.15	3.35	98.72	286	83	772	67	483	33	0.1383
165Uii	13.0	S	41.3	1.19	30.7	0.03	11.91	3.52	0.46	1.44	1.44	4.14	0.03	3.80	100.22	230	117	845	73	530	29	0.1473
165Gi	17.0	S	41.4	1.54	29.2	0.03	12.02	4.16	0.34	1.46	1.86	3.95	0.09	2.90	99.23	237	150	676	53	400	29	0.1094
165Gii	18.0	WS	56.3	1.08	20.1	0.02	8.05	3.11	0.17	1.32	2.31	3.80	0.05	2.60	99.09	176	179	749	39	302	18	0.0822
165Fi	19.0	WS	63.0	0.95	17.9	0.02	6.48	2.89	0.10	0.92	1.42	3.99	0.11	2.55	100.57	190	128	913	29	272	16	0.0721
165H	21.0	WS	57.9	1.02	18.6	0.02	8.23	3.20	0.13	0.91	1.23	4.38	0.11	2.85	98.76	188	120	846	36	288	16	0.0831
165Fii	24.0	WS	62.8	0.92	17.5	0.02	6.34	2.74	0.11	0.88	1.31	4.10	0.12	2.35	99.34	171	118	806	32	253	16	0.0700
165Fiii	26.0	WS	60.4	1.00	18.7	0.02	6.99	3.11	0.11	1.00	1.68	4.15	0.10	2.60	100.13	177	141	844	30	281	16	0.0734
Site 165 North
165A	1.0	S	39.7	1.44	27.2	0.02	11.59	4.50	0.27	0.72	0.76	7.33	0.03	4.15	99.06	304	82	1440	48	305	31	0.0973
165V	1.0	S	41.4	1.60	30.7	0.03	12.23	4.65	0.18	0.78	0.52	4.17	0.16	2.10	98.83	250	53	565	60	313	29	0.1126
165Li	4.0	S	40.6	1.58	28.0	0.03	12.30	3.98	0.40	1.46	1.37	5.55	0.21	3.05	98.78	249	129	1060	55	371	25	0.1141
165Lii	7.0	S	40.5	1.55	27.9	0.03	12.44	4.06	0.39	1.46	1.29	5.48	0.24	3.05	98.66	261	123	1090	49	348	28	0.1070
165Oi	9.5	S	41.2	1.43	28.0	0.03	11.59	4.69	0.22	1.03	1.08	5.97	0.22	3.75	99.51	296	112	1160	40	281	21	0.0946
165Oii	13.5	S	41.7	1.35	29.1	0.02	10.50	4.55	0.12	0.64	0.86	6.38	0.17	3.85	99.60	288	98	1150	36	251	22	0.0900
165Oiii	17.5	S	51.2	1.06	22.9	0.02	9.27	3.84	0.14	1.50	2.37	4.52	0.14	2.80	100.03	214	200	800	36	240	17	0.0798
165Ii	17.5	S	49.1	1.36	25.5	0.02	9.45	2.91	0.15	0.86	1.31	4.58	0.13	3.50	99.21	187	125	927	50	321	24	0.1123
165M	30.0	WS	59.2	1.04	20.5	0.01	6.55	2.38	0.14	0.91	1.45	4.54	0.10	2.60	99.64	167	145	804	38	254	20	0.0831
165Iii	37.5	WS	57.9	1.07	20.7	0.01	6.50	2.44	0.10	0.68	1.19	5.09	0.10	3.10	99.15	176	125	1000	39	258	19	0.0846
165J	49.0	WS	70.1	0.71	14.4	b.d.	4.51	1.84	0.06	0.49	0.88	3.51	0.07	2.60	99.33	136	92	758	25	183	14	0.0582
Site 114
114o	1.1	S	43.6	0.98	26.6	0.03	14.65	5.29	0.91	1.97	0.21	3.29	0.21	1.60	99.58	174	23	454	53	276	12	0.0828
114i	0.9	S	41.5	1.11	32.4	0.03	12.94	4.89	0.62	1.51	0.17	3.09	0.02	1.35	99.79	157	18	357	41	313	26	0.0875
114ii	2.3	S	39.2	1.59	30.4	0.03	13.97	6.31	0.68	1.35	0.16	4.14	0.02	1.50	99.50	215	18	463	41	344	26	0.0987
114iii	2.4	S	39.1	1.65	29.2	0.03	14.02	6.82	0.63	1.24	0.04	4.53	0.02	1.80	99.41	226	19	539	44	363	26	0.1131
114iv	4.0	S	59.0	0.95	18.5	0.02	7.88	4.16	0.30	1.29	0.99	3.74	0.12	2.00	99.13	171	70	557	25	207	15	0.0618
114v	6.5	WS	56.6	0.96	19.2	0.02	8.36	4.46	0.24	0.78	0.66	4.99	0.13	2.15	98.76	190	64	889	21	201	14	0.0586
114vi	11.0	WS	60.6	0.94	18.0	0.02	6.68	3.96	0.21	0.60	0.51	5.15	0.14	2.35	99.37	184	62	1050	23	213	16	0.0620

Notes: Concentrations in wt% except traces in parts per million. All Fe as Fe₂O₃. LOI = loss on ignition. Totals include Rb, Sr, Ba, Y, Zr, Nb, Ce, and V summed as oxides. *wRE* calculated as described in text using Zr, Th, and U wt%. Distances *x* are in cm from quartz vein-selvage contacts. S = selvage, WS = wallrock schist. 114o lies on the opposite side of the vein from the 114i-114vi traverse. b.d. = below detection. Concentrations determined by XRF methods except Y by ICP-MS.

wallrock outside the selvages is somewhat arbitrary. Here, the selvages are defined based on their strongly depleted silica contents and coarse grain size relative to rocks more far removed from veins (Fig. 2d). The grain size increases can be quite striking; Figure 4 illustrates strong increases in kyanite crystal lengths toward the veins at both sites 114 and 165. The above criteria are sufficient for general delineation of the selvages, but the reader should keep in mind that each element will have a different characteristic transport distance (Bickle 1992), such that no single length scale can describe all the metasomatic behavior. It is worthwhile to note that

although selvages can be visually distinguished in strongly weathered outcrops (Fig. 2), they are much less obvious in fresher natural exposures or in road cuts.

Chemical analyses were done by SGS Minerals services using standard X-ray fluorescence (XRF) and inductively coupled plasma-mass spectrometer (ICP-MS) techniques (Tables 1 and 2; for summaries of techniques and analytical precision, see Ague 1994a, 2003a; Bucholz and Ague 2010). Representative bulk vein analyses were precluded by the coarse-grained nature and very irregular distribution of vein kyanite, and by the common occurrence of wallrock inclusions.
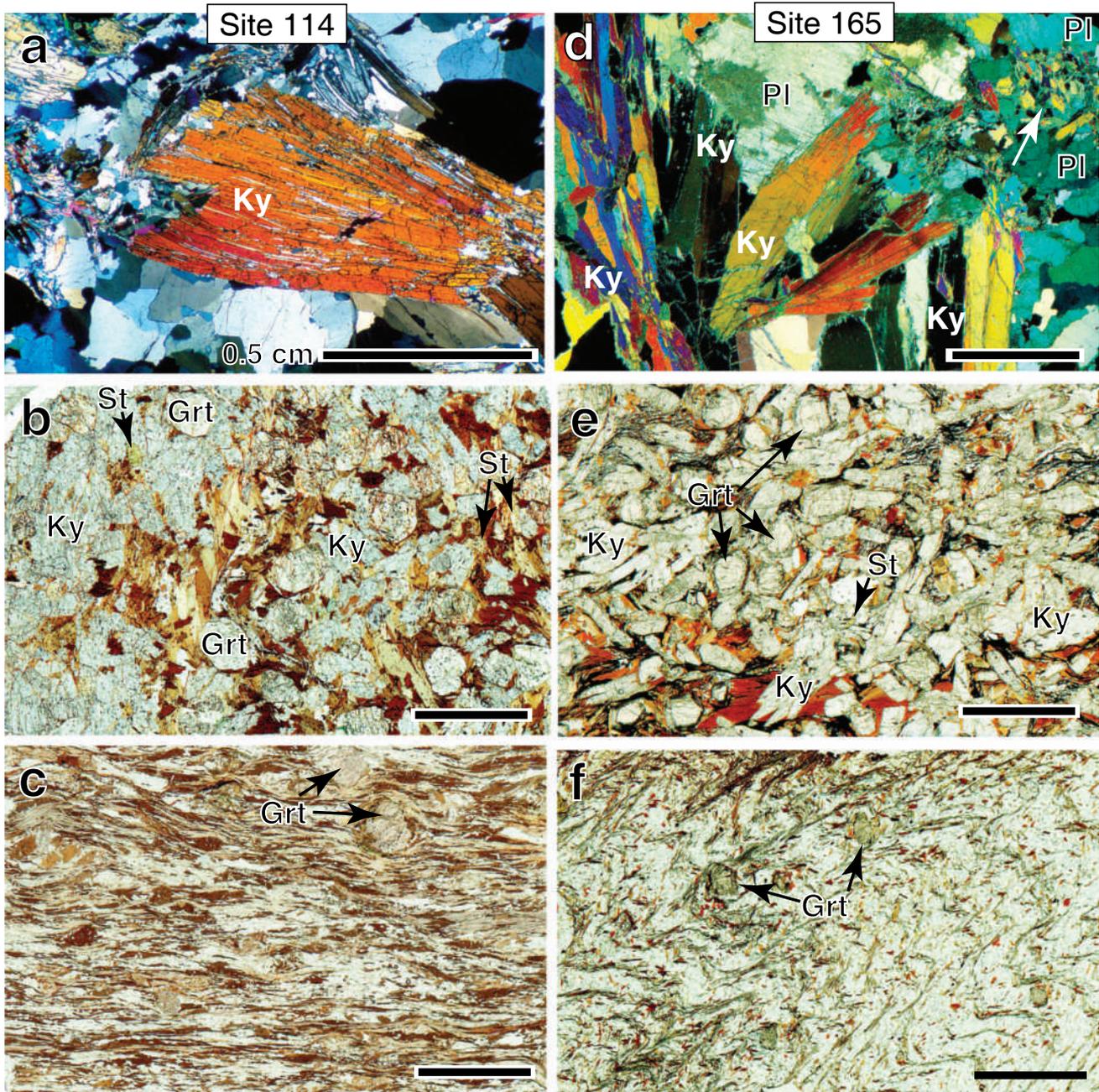
FIGURE 3. Photomicrographs. Parts (**a**) and (**d**) under crossed polars; remainder under plane-polarized light. Scale bars = 0.5 cm. Parts (**a–c**) Vein-selvage relations, site 114. (**a**) Large kyanite (Ky) blades in quartz vein. (**b**) Kyanite- and garnet-rich (Grt) selvage. Staurolite (St) and biotite (dark) also present. Abundant dark "specks" in the photo are mostly rutile and zircon crystals, concentrated due to silica loss. (**c**) Wallrock schist distal to veins rich in quartz and plagioclase (light) and bands of muscovite + biotite. Parts (**d–f**) Vein-selvage relations, site 165. (**d**) Kyanite blades cutting slightly sericitized, pre-existing plagioclase (Pl) in vein. Arrow denotes plagioclase almost completely replaced by small kyanite crystals (light). (**e**) Kyanite- and garnet-rich selvage. Biotite (dark) also present. Concentrations of organic matter in bands and between grains appear black. (**f**) Wallrock schist distal to vein is dominated by contorted quartzofeldspathic (light) and muscovite+biotite bands.

MASS BALANCE ANALYSIS

Successful mass balance analysis of chemical mass transfer proceeds as follows. (1) The altered rocks are compared geochemically to less altered "precursor" rocks. The less altered rocks must have the same composition the altered rocks did
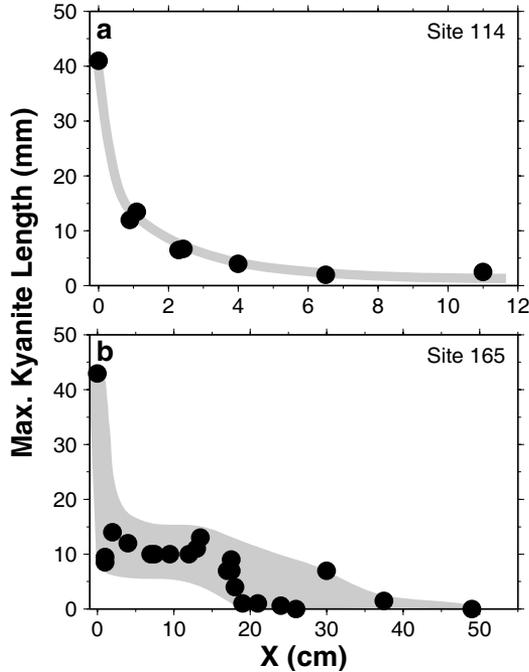
FIGURE 4. Maximum length of kyanite crystals measured in hand specimen as a function of distance from quartz veins for (**a**) site 114 and (**b**) site 165.

prior to metasomatism. In the present study, the veins cut single metapelitic layers. Consequently, there is no doubt that the selvages are the altered rocks derived from the less altered wallrock schists that lie beyond the selvage margins. (2) A reference frame for quantitatively determining changes in mass and volume must be identified. This could be constant rock mass, constant rock volume, or constant mass of reference elements (Gresens 1967; Grant 1986; Brimhall et al. 1988; Ague and van Haren 1996). The last choice is the most general and can account for all scenarios, including constant rock mass or volume.

The choice of the low-solubility element or elements for the geochemical reference frame must take into account petrological, mineralogical, and geochemical data and observations. Titanium is often used, but rutile in veins indicates some degree of Ti mobility; the transport of Ti has been documented in other settings as well (e.g., Selverstone et al. 1992; Franz et al. 2001; Ague 2003a; Jiang et al. 2005; Gao et al. 2007). The concentration of Al in solutions coexisting with kyanite and quartz can be significant at high *P-T* conditions leading to Al mass transfer (cf. Nabelek 1997; Manning 2006; Sepahi et al. 2006). Kyanite was precipitated in the veins, ruling out Al as a reference frame element. In contrast, zircon grains, the primary hosts for Zr, vary little in morphology across the profiles and are not found in the veins. In general, they have exceedingly low solubilities in typical metamorphic fluids and do not undergo extensive modification at Barrovian pressures until partial melting conditions are reached. Zr/Th and Zr/U ratios for the less altered wallrock schists beyond the selvage margins are the same, within error, as those for selvages; thus, Zr, Th, and U were used to calculate mass change values (see below). Thorium is known to be highly immobile in aqueous fluids (cf. Johnson and Plank 1999). Uranium can be mobile under oxidizing conditions, but the near

TABLE 2. Trace elements

	x(cm)	Type	Cs	La	Ce	Pr	Nd	Sm	Eu	Gd	Tb	Dy	Ho	Er	Tm	Yb	Lu	Th	U	Pb	V	Co	Ni	Cu	Zn	Sn	Hf	Li
													Site 165 South															
165B	2.0	S	9.6	73.9	157	18.1	68.2	12.0	1.94	12.10	1.96	11.4	2.31	6.94	1.11	7.9	1.18	22.8	5.37	16	147	16.3	42	21	28	1	11	115
165C	12.0	S	15.9	96.5	204	23.5	85.7	15.3	2.59	11.70	2.10	11.9	2.56	7.68	1.08	7.6	1.02	29.8	6.73	19	249	27.5	65	45	102	3	13	148
165Uii	13.0	S	11.8	91.8	193	21.8	82.0	14.2	2.42	11.30	2.19	13.4	2.82	8.72	1.46	10.5	1.53	29.1	7.53	31	202	16.3	37	13	42	3	14	102
165Gi	17.0	S	13.1	71.1	148	18.5	64.7	12.2	2.30	11.00	1.89	10.3	2.17	6.25	0.99	6.7	1.03	22.2	5.36	29	210	29.1	73	46	216	3	10	175
165Gii	18.0	WS	9.1	53.7	112	13.1	48.6	8.4	2.06	6.93	1.34	7.59	1.58	4.66	0.70	4.8	0.71	17.0	3.94	33	159	17.4	50	13	67	3	8	84
165Fi	19.0	WS	8.9	45.8	93.9	10.9	41.4	7.3	1.66	6.08	1.09	6.04	1.23	3.51	0.53	3.6	0.54	14.2	3.51	29	139	21.1	71	19	36	3	6	57
165H	21.0	WS	9.0	48.9	118	13.7	43.0	7.5	1.92	6.73	1.29	7.27	1.43	4.48	0.64	4.2	0.62	17.6	4.15	31	148	39.8	92	47	88	3	7	93
165Fii	24.0	WS	8.7	46.1	95.9	11.0	41.6	7.7	1.56	6.17	1.11	6.21	1.25	3.61	0.55	3.6	0.52	14.6	3.39	25	129	20.6	58	17	50	3	6	74
165Fiii	26.0	WS	9.1	46.1	97.2	11.4	43.6	7.5	1.71	6.03	1.09	6.33	1.29	3.60	0.55	3.6	0.59	14.1	3.59	27	144	22.3	62	20	41	3	7	71
													Site 165 North															
165A	1.0	S	13.5	68.0	146	16.7	62.2	12.0	2.01	9.42	1.78	10.6	2.14	5.70	0.94	6.4	0.99	21.4	5.15	25	247	23.5	57	26	48	5	8	108
165V	1.0	S	15.3	82.8	174	20.1	76.6	14.6	2.26	11.60	2.07	12.2	2.51	7.21	1.07	7.2	1.10	25.9	6.30	17	224	36.6	105	58	483	3	8	300
165Li	4.0	S	12.9	77.7	164	19.0	73.6	14.3	2.65	11.40	2.03	11.2	2.23	6.62	1.02	6.8	1.02	25.1	5.85	30	220	26.1	100	48	90	4	9	115
165Lii	7.0	S	13.0	75.5	159	18.3	70.3	13.5	2.52	11.20	2.02	10.4	2.05	6.06	0.93	6.4	0.95	23.4	5.51	28	214	27.9	108	53	85	4	9	112
165Oi	9.5	S	14.4	77.1	162	18.8	70.5	13.0	2.38	9.99	1.73	8.99	1.68	4.85	0.75	5.2	0.80	22.0	4.97	28	215	30.7	100	42	147	4	7	155
165Oii	13.5	S	13.1	71.1	148	16.7	62.4	11.0	2.16	8.50	1.54	7.71	1.48	4.03	0.65	4.4	0.65	22.3	4.67	28	232	35.5	97	35	308	5	6	223
165Oiii	17.5	S	10.7	58.7	121	13.9	54.1	9.5	2.27	7.37	1.35	7.55	1.51	4.30	0.65	4.4	0.72	18.6	4.14	37	165	30.4	74	39	90	3	6	116
165Ii	17.5	S	8.5	75.9	174	20.1	72.3	13.3	2.44	10.50	1.90	10.2	2.06	5.87	0.87	5.6	0.83	27.1	5.88	31	186	47.3	98	87	234	3	8	151
165M	30.0	WS	7.6	56.8	119	13.8	50.9	8.8	1.95	6.81	1.38	7.76	1.50	4.42	0.65	3.9	0.61	19.1	4.32	32	151	20.7	46	49	35	5	6	65
165Iii	37.5	WS	7.1	60.8	128	14.7	55.1	9.5	2.08	9.41	1.42	7.88	1.62	4.08	0.69	4.3	0.61	20.1	4.25	32	159	21.0	57	39	43	4	6	61
165J	49.0	WS	5.7	40.6	84.8	9.66	36.2	6.4	1.36	5.13	0.91	5.01	1.01	2.93	0.40	2.8	0.42	13.3	2.96	24	103	13.8	29	24	22	2	4	46
													Site 114															
114o	1.1	S	6.6	20.6	79.8	5.92	22.6	5.0	1.17	5.07	1.46	10.0	2.16	6.35	0.97	6.4	0.98	18.7	4.03	10	138	34.5	112	14	120	2	8	128
114i	0.9	S	6.1	25.5	73.6	7.06	26.7	5.6	1.23	4.99	1.25	8.16	1.77	5.57	0.86	6.3	0.91	19.3	4.05	11	138	30.4	91	25	92	2	8	143
114ii	2.3	S	8.9	24.6	74.6	7.07	26.1	5.5	1.32	4.94	1.18	8.15	1.72	5.21	0.86	5.9	0.94	23.7	4.28	10	174	38.9	131	10	119	3	9	153
114iii	2.4	S	9.7	36.9	112	10.6	32.3	7.8	1.92	6.85	1.53	9.58	1.98	5.77	0.92	6.5	0.90	29.9	4.75	12	189	41.9	145	9	147	3	10	160
114iv	4.0	S	6.2	25.1	63.2	7.53	29.5	6.0	1.21	4.66	0.95	5.56	1.16	3.21	0.51	3.3	0.51	14.0	2.99	24	145	25.9	92	b.d.	179	3	5	111
114v	6.5	WS	7.4	8.8	25.7	2.73	9.6	2.0	0.48	1.76	0.51	3.98	0.91	2.60	0.43	3.2	0.41	14.3	2.53	26	160	24.5	90	24	67	3	5	86
114vi	11.0	WS	5.6	39.6	79.5	10.3	38.4	7.4	1.50	5.47	0.94	5.34	1.01	2.99	0.44	2.8	0.43	14.3	2.86	32	156	25.3	84	6	63	4	5	71

Notes: Concentrations (ppm) determined by ICP-MS. Distances *x* are in cm from quartz vein-selvage contacts. S = selvage, WS = wallrock schist. 114o lies on the opposite side of the vein from the 114i-114vi traverse. b.d. = below detection.

ubiquitous presence of organic matter in the Wepawaug would have maintained low oxygen fugacities. The fluids contained CO_2 and other carbon species (Ague 2003a), but in general CO_2 and CH_4 are poor solvents compared to water (e.g., Newton and Manning 2000), thus *decreasing* the solubility of common silicate minerals like quartz and, most likely, zircon as well.

The equations for mass and volume change follow from Ague (1994a; see also references therein). The total rock mass change based on reference species i is

$$T_{mass,i} = \left(\frac{C_i^0}{C_i'}\right) - 1 \tag{1}$$

where $T_{mass,i}$ is the mass change (multiplication by 100 yields the percentage mass change). C is concentration and the superscripts ^{0} and $'$ denote wallrock schist and altered rock (selvage), respectively. The choice of concentration units is arbitrary; wt% element is used herein. Mass gains are positive, and mass losses are negative. The volume strain estimated using reference species i is

$$\varepsilon_i = \left(\frac{C_i^0}{C_i'}\right)\left(\frac{\rho^0}{\rho'}\right) - 1 \tag{2}$$

where ε_i is volume strain and ρ is bulk rock density. Porosity can also be a factor but is not considered here as it has a negligible impact on strain estimates if it is small and/or if the wallrock schist and selvage porosities were similar during mass transfer (Ague 1994a).

The mass change for mobile species j estimated using reference species i is

$$\tau_i^j = \left(\frac{C_i^0}{C_j^0}\right)\left(\frac{C_j'}{C_i'}\right) - 1 \tag{3}$$

where τ_i^j is the fractional mass change. Statistical analysis of mass changes is generally necessary due variations in wallrock schist compositions and the intensity of mass transfer; modern analytical errors are in general small relative to these other factors. A method that takes into account the complications inherent in the statistical analysis of compositional data sets gives the average or "most probable" mass change value as (Ague 1994a):

$$\hat{\tau}_i^j = \exp\left(ML^0 + ML' \pm 2\sigma\right) - 1 \tag{4}$$

where ML denotes the mean of the logarithms of the concentration ratios and σ is the standard error. The ML values are calculated using

$$ML^0 = \frac{1}{N^0}\sum_{n=1}^{N^0} \ln\left(\frac{C_{i,n}^0}{C_{j,n}^0}\right) \tag{5}$$

$$ML' = \frac{1}{N'}\sum_{n=1}^{N'} \ln\left(\frac{C_{j,n}'}{C_{i,n}'}\right) \tag{6}$$

where N^0 and N' are the total number of wallrock schist and altered selvage samples, respectively. The use of ratios circum-

vents the "closure problem," and the geometric means are a way to account for the often strongly non-Gaussian distributions of compositional ratio data (Aitchison 1986; Woronow and Love 1990; Ague and van Haren 1996). Standard statistical Student's t distribution tests may then be used to assess whether the mean logratios for wallrock schists (Eq. 5) and altered rocks (Eq. 6) are different at the 95% confidence level; tests are available for cases where the variances on the two means are equal or unequal (cf. Spiegel 1961). The standard error on τ_i^j is estimated by summing the standard errors on ML^0 and ML' in quadrature:

$$\sigma = \left[\left(\frac{s_{ML^0}}{\sqrt{N^0}}\right)^2 + \left(\frac{s_{ML'}}{\sqrt{N'}}\right)^2\right]^{1/2} \tag{7}$$

where the s terms denote the sample standard deviations on ML^0 and ML'.

Low-solubility, high-field strength elements (HFSE) like Zr are commonly employed to define the geochemical reference frame. A complicating factor is that sedimentary rocks are heterogeneous to some extent, even within single layers, resulting in variability in the chemical compositions of wallrock schists. This variability can be "smoothed out" to some degree by using more than one element to define the geochemical reference frame (e.g., Grant 1986; Baumgartner and Olsen 1995). One way to proceed is to use the sum of the concentrations of reference species (cf. Ague and van Haren 1996). However, different elements can have vastly different concentrations, so this method weights the result toward those elements that have the highest concentrations. To avoid this problem, the use of a weighted sum of reference species concentrations is proposed here so that each element contributes equally:

$$wRE = C_1 + \sum_{k=2}^{K} \frac{M_1}{M_k} C_k \tag{8}$$

where wRE is the weighted residual element sum, k is an index, K is the total number of reference species, C_k is the concentration of species k, and M_k is the mean concentration of k for the entire sample set. As discussed above, in this study the HFSE Zr, Th, and U are used to define the geochemical reference frame. Taking the concentration of Zr as C_1, the value of wRE^0 for each wallrock schist sample n is calculated as:

$$wRE_n^0 = C_{Zr,n}^0 + \frac{M_{Zr}}{M_{Th}}C_{Th,n}^0 + \frac{M_{Zr}}{M_U}C_{U,n}^0 . \tag{9}$$

An analogous procedure is used for each altered sample. The choice of which element is taken for C_1, C_2, etc., is arbitrary. Both the geometric and the standard arithmetic mean were investigated for calculating the M_i values; the results were found to be nearly identical so the arithmetic mean was used herein. Mass changes and uncertainties for mobile constituents, j, were calculated by substituting wRE^0 and wRE' for the C_i^0 and C_i' terms in Equations 1–6.

The selvages lost silica as a result of mass transfer to adjacent veins. The percentage mass loss (and 2σ range) calculated using Zr alone as the reference frame is: 47.1% (34.9 to 57.1%);

for Th alone it is: 51.4% (41.7 to 59.6%); and for U alone it is: 50.9% (40.1 to 59.8%). All estimates are very similar but, a priori, there is no definitive way to discern which of them is the "best." Using *wRE* as the reference yields a mass loss of: 49.9% (39.6 to 58.5%). Thus, the *wRE* reference can be thought of as providing an "average" result that weights each reference species equally.

RESULTS

Wedge diagrams

Elements may be gained, lost, or remain immobile during metasomatism. "Wedge diagrams" are a simple way to assess these changes (Ague 1994a). The geochemical reference is plotted on the *x*-axis, and a potentially mobile element is plot-
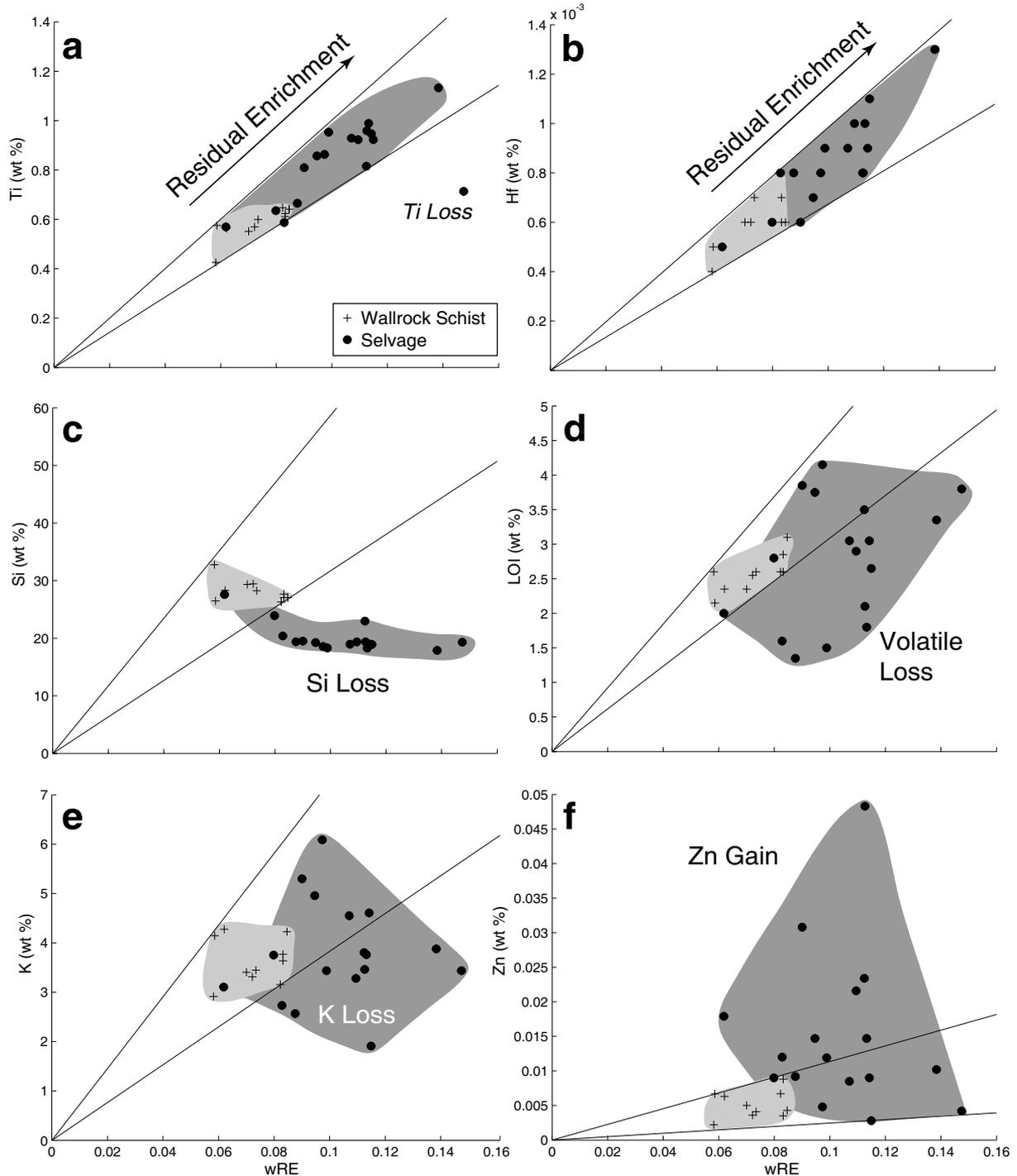
FIGURE 5. Wedge diagrams. *wRE* is weighted residual element value computed using Equation 8 in the text. Concentrations are given in terms of wt% element, except for LOI (loss on ignition), which is given as total wt%. (**a**) Ti. (**b**) Hf. (**c**) Si. (**d**) LOI, a proxy for rock volatile content. (**e**) K. (**f**) Zn.

ted on the y-axis. The compositional data for the wallrock schist samples will define a field of points; variability is caused by, for example, original chemical heterogeneities in the rocks. Drawing two lines from the outer edges of the field through the origin defines a wedge-shaped region (Fig. 5). If the y-axis element was immobile, or nearly so, then data for the altered selvage rocks must lie within the wedge. In this case, if rock mass was lost overall, then both the x- and y-axis elements undergo "residual enrichment" due to the loss of other constituents. On the other hand, such elements undergo "residual dilution" if rock mass was gained. For a mobile y-axis element, the data field for altered rocks will extend above the wedge if the element was gained, or below the wedge if lost.

Mass changes as well as residual behavior are apparent in the data set. When plotted against the *wRE* reference, nearly all the Ti and Hf data for altered samples lie within the wedge on the trend expected for residual enrichment (Figs. 5a and 5b). Consequently, these elements, along with the Zr, Th, and U making up the *wRE* reference, almost certainly underwent little fluid-driven mass transfer during metamorphism. The exception is one selvage sample that clearly falls below the Ti wedge indicating Ti loss (Fig. 5a). Limited local transfer of Ti from selvages to veins could explain the traces of rutile found in some veins. However, such transfer appears to have been rare (Fig. 5a), so it is possible that some vein rutile crystals are simply refractory xenocrysts mechanically incorporated into the fractures during deformation.

Silica, LOI (loss on ignition, a proxy for volatiles), K, and Zn behavior differs markedly from that of the residual elements. The Si data for selvage samples define an array extending from the little-altered wallrock schist field into the region of mass loss (Fig. 5c). Major silica transfer from selvages to veins was a key part of vein formation in the Wepawaug (Ague 1994b); the considerable residual enrichment of Zr, Th, U, Ti, Hf, and related elements in selvages (Figs. 5a and 5b) is due largely to this silica loss. Although there is some scatter, on average it is clear that volatiles (LOI) and K were lost from selvages (Figs. 5d and 5e). On the other hand, significant Zn gains are recorded by some selvage samples (Fig. 5f). The loss of volatiles is consistent with the observed increases in abundances of kyanite, garnet, and staurolite at the expense of micas (particularly muscovite) in the selvages (Fig. 3).

Average mass changes

The mean percentage mass changes ($\hat{\tau}_i$; Eq. 4) needed to produce the selvages from the wallrock schists are shown in Figure 6. Those constituents whose difference in logratio means (Eqs. 5 and 6) is significant at the 95% confidence level are considered to have undergone mass transfer. It follows that the 2σ error bounds for such constituents calculated using Equations 4–7 do not overlap zero on Figure 6. Note, however, that 2σ underestimates 95% confidence intervals somewhat for "small" sample sizes less than about 30 (in this study, $N^0 = 10$ and $N' = 17$). Consequently, when assessing differences between means
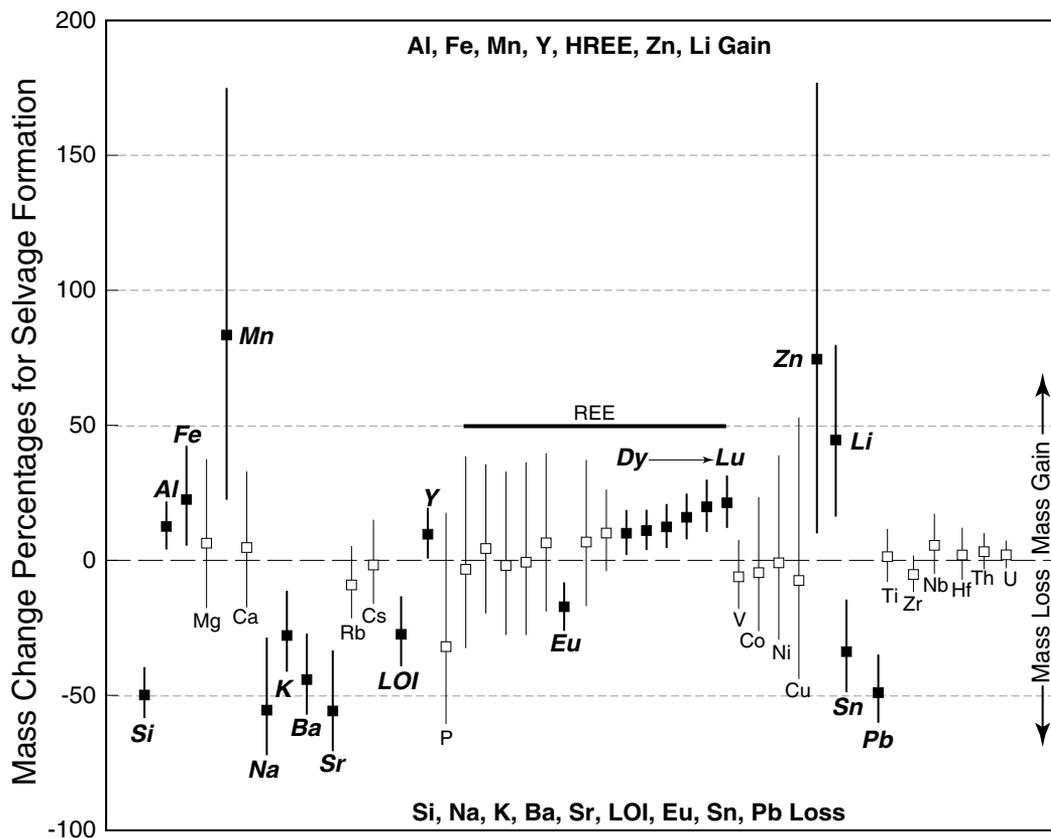
FIGURE 6. Mass changes percentages for selvage formation. Negative values indicate mass loss, whereas positive values indicate mass gain. Uncertainties are 2σ. Elements shown with filled symbols have statistically significant (95% confidence) mass changes. Computed by excluding the Al and Eu values for the wallrock schist sample closest to a vein (114v), as this sample has undergone considerable mass transfer for some elements (see text).

at a specified confidence level, it is essential to use methods based on Student's *t* distribution because such methods account for small sample size effects (cf. Spiegel 1961). HFSE elements including Zr, Th, U, Ti, Hf, and Nb cluster tightly around the 0% mass change line. On average, Si, Na, K, Ba, Sr, volatiles (LOI), Eu, Pb, and Sn were all lost; mass loss values range from about 25% to 60%. On the other hand, Al, Fe, Mn, heavy rare earth elements (HREE), Zn, Li, and Y were gained. Phosphorous underwent local gains and losses; however, on average, there was no statistically significant mass transfer of P into or out of the selvages (see below).

Equation 1 can be used to evaluate whether mass gains or losses dominated the overall mass transfer. The average *wRE* values for wallrock schists and selvages are 0.0752 and 0.102, respectively; the mean mass change associated with selvage formation is thus –26% (the geometric mean produces the same result). Consequently, mass losses dominated the mass transfer, consistent with the residual enrichment trends depicted in Figures 5a and 5b. As noted above and in Ague (1994b), the bulk of this mass change was due to silica loss.

Geochemical profiles

The wedge and mass change diagrams convey the average sense of mass transfer, but do not show the spatial relationships between samples. Consequently, geochemical data for each sampling traverse are illustrated as a function of distance from the quartz veins in Figures 7–9. The mass change systematics are similar for each of the three traverses; therefore, all the samples are combined on each graph.

If Ti and Hf were largely immobile, then Ti/*wRE* and Hf/*wRE* ratios should remain constant regardless of distance from the veins. As this is indeed the case (Figs. 7a and 7b), little mass transfer of these elements probably occurred, consistent with the wedge diagrams (Figs. 5a and 5b). As discussed above, one sample lost Ti, and it plots at a noticeably lower Ti/*wRE* ratio on Figure 7a.

The mass change diagram (Fig. 6) shows, on average, that Al, Fe, Mn, and Zn were gained by the vein selvages. The geochemical profiles clearly illustrate upturns in the Al/*wRE*, Fe/*wRE*, Mn/*wRE*, and Zn/*wRE* ratios as the veins are approached (Figs. 7c–7f). Because *wRE* is the reference frame, an increase in ratio corresponds to mass gain. Interestingly, the wallrock schist samples closest to the veins also underwent mass addition, particularly with respect to Al and Fe (Figs. 7c and 7d). Consequently, mass changes can extend beyond the limits of major silica depletion used in a general way here to define selvage boundaries. There is some scatter in the data, but they do show that the zone of pronounced Mn addition is thinner than those for the other elements (Figs. 7c–7f).

Na/Ca and Sr/Rb ratios both decrease noticeably toward the veins (Figs. 8a and 8b). For Na/Ca, this decrease is due mostly to the Na loss illustrated by the mass change diagram (Fig. 6). In addition, although the average Ca mass change in not statistically significant (Fig. 6), the samples nearest the veins tend to have the highest Ca/*wRE* ratios, possibly indicating some mass addition (not shown). This too would contribute to the large deceases in Na/Ca toward the veins. The decrease in Sr/Rb is due to Sr loss; Rb mass changes were not statistically significant (Fig. 6).

The ratios Al/Na and Al/K increase markedly as the veins

are approached (Figs. 8c and 8d). Note that this conclusion is unequivocal and does not depend on the geochemical reference frame chosen. The ratios increase due to simultaneous gains of Al and losses of K and Na (Figs. 5e, 6, 7c, and 8a). The strong increases in the aluminous nature of the selvages undoubtedly helped to stabilize and foster the growth of the aluminous index minerals kyanite and staurolite (cf. Ague 1994b).

Rare earth elements were shown to be mobile during metamorphism of metacarbonate rocks in the Wepawaug Schist (Ague 2003a). As illustrated in Figures 6, 8e–8f, and 9a, they were also mobile during metamorphism of the metapelites. Interestingly, although heterogeneities in the composition of the original sediments and/or degree of alteration make it impossible to distinguish average mass changes for Sm and Nd in Figure 6, their ratio clearly increases toward the veins (Fig. 8e). As a result, one or both elements must have been mobile. Mass additions of HREE like Yb are easily distinguishable on the mass change diagram (Fig. 6); as expected, the Yb/*wRE* ratio increases significantly toward the veins, reflecting Yb mass gain in the selvages (Fig. 8f). In contrast, the Eu/wRE ratio drops precipitously toward the veins, indicating overall mass loss (Fig. 9a). Note that the wallrock schist sample closest to a vein actually has the lowest ratio (114v). As noted above, the designation of "wallrock schist" or "selvage" based on the level of silica depletion and porphyroblast grain size is somewhat arbitrary; clearly, mass transfer of elements like Eu could extend beyond the limits of the silica-depleted vein margins. The advantage of plotting geochemical relationships as functions of distance from veins is that mass transfer effects are shown in their proper spatial context, regardless of what name designation a particular sample is given.

Lead and Li were also mobile. U/Pb ratios increase by a factor of ~3 toward the veins (Fig. 9b). As U was relatively immobile, the increase in ratio is due to the loss of Pb (Fig. 6). Similarly, Th/Pb ratios increase by a factor of ~5 (not shown). Unlike Pb, which was lost from the selvages, Li was gained, as indicated by the increases in Li/*wRE* values as the veins are approached (Fig. 9c).

The behavior of phosphorous differs from that of the other elements discussed thus far. Relative to wallrock schists, some selvage samples have large P/*wRE* ratios, suggesting mass gains, whereas others have low ratios (Fig. 9d). These relationships indicate that P was locally mobile—being gained in some areas and lost from others—but overall there were no statistically distinguishable net gains or losses (Fig. 6). Similar P systematics in selvages adjacent to quartz-kyanite veins in the Barrovian rocks of Unst, Shetland Islands, Scotland, were described by Bucholz and Ague (2010).

DISCUSSION

Silica mass transfer and vein formation

One of the most striking mass changes is the loss of quartz from the selvages. If all the silica in the veins was locally derived from the adjacent selvages, then the amount of silica lost from the selvages will account for the vein mass. If not, then some proportion of the silica must have been externally derived from through-going fluids (here, *external* refers to outside the local selvage–wallrock schist system). The amounts of internally derived and externally derived silica can be approximated by mass
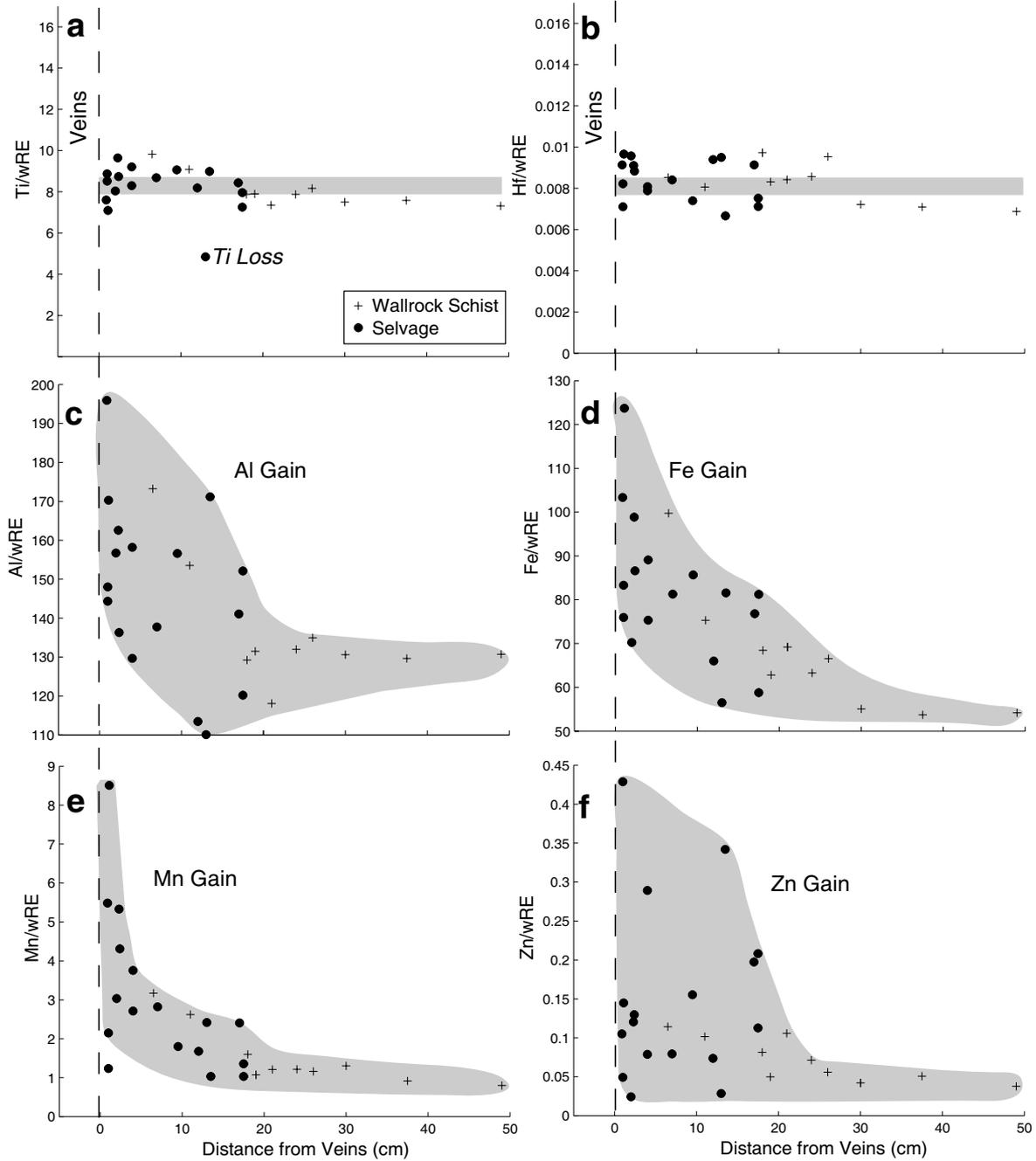
FIGURE 7. Geochemical profiles. Data for all three traverses plotted on the same *x*-axis. (**a**) Ti/*wRE*. Near constant ratio across profiles indicates little overall mass transfer of Ti, except for one sample that has a noticeably lower ratio and may have lost Ti (see text). Horizontal line shown for reference. (**b**) Hf/*wRE*. Near constant ratio across profiles indicates little if any mass transfer of Hf. Horizontal line shown for reference. (**c**) Al/*wRE*. Note increases in Al/*wRE* toward veins. Increase in an element's concentration relative to *wRE* reference frame indicates mass addition. (**d**) Fe/*wRE*. (**e**) Mn/*wRE*. (**e**) Zn/*wRE*.

balance given observed vein and selvage thicknesses under the reasonable assumptions that all volume strain and mass transfer occurred perpendicular to vein-selvage contacts, and that the veins can be approximately modeled as pure quartz.

The volume strain is needed to estimate the original thicknesses of the selvages (Eq. 2). The reference ratio wRE^0/wRE' is 0.0752/0.102 = 0.74. The average densities of wallrock schist and selvage were taken to be 2800 and 3100 kg/m³, respectively

(Ague 1994a 1994b). The resulting mean volume loss is 34%. For site 114, the selvages are 4 cm wide and the vein is 4.25 cm wide. Given an average wallrock schist SiO_2 content of 60.5 wt% and 50% mass loss of silica from the selvages, the amount of silica removed from the two selvages on either side of the vein would produce a vein 3.4 cm wide. Thus, we estimate that 80% of the vein was derived from local silica transfer from the selvages, and 20% was externally derived from fluids. The vein at site 165 is
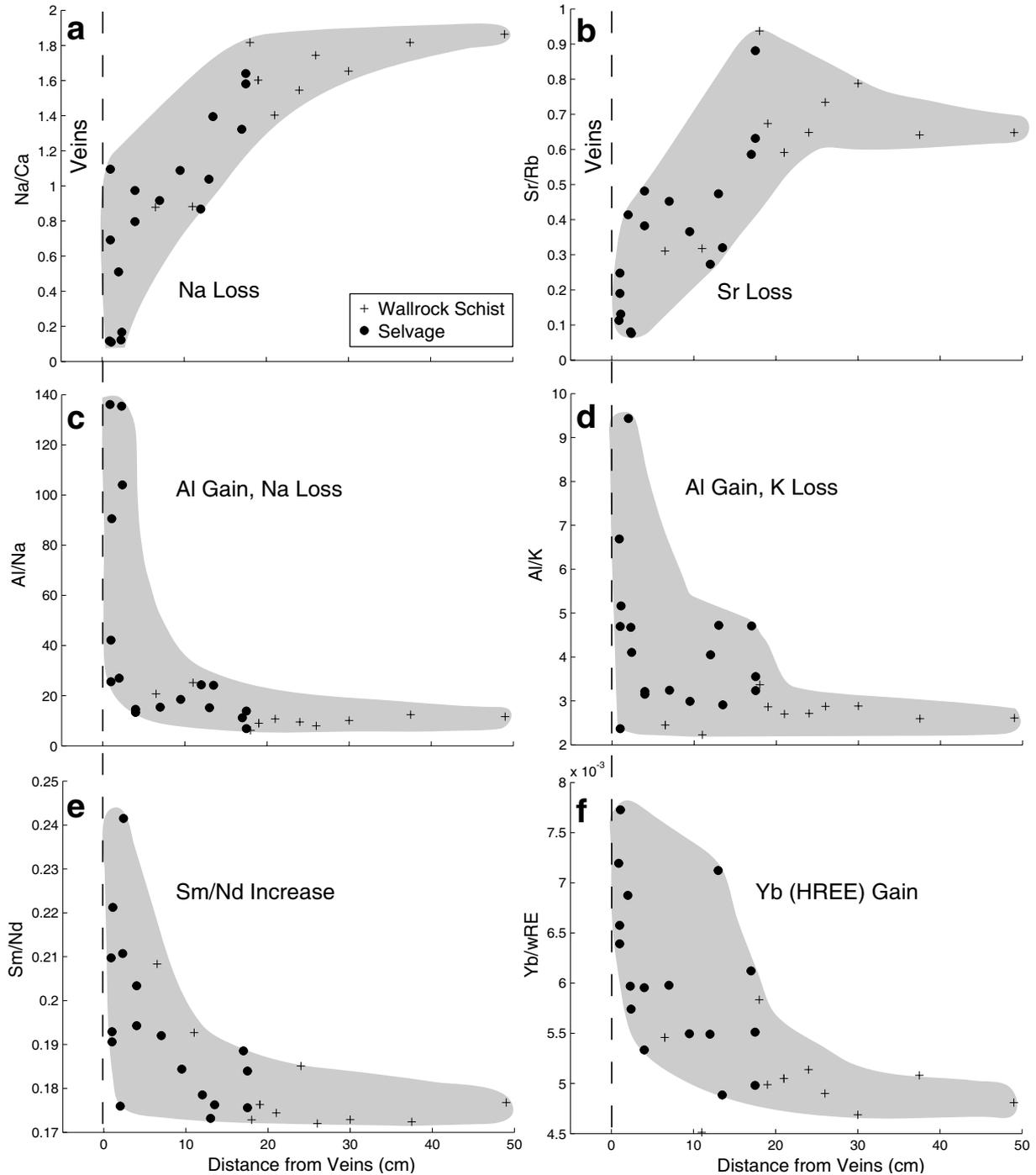
FIGURE 8. Geochemical profiles. Data for all three traverses plotted on the same *x*-axis. (**a**) Na/Ca. (**b**) Sr/Rb. (**c**) Al/Na. (**d**) Al/K. (**e**) Sm/Nd. (**e**) Yb/*wRE*.

40 cm wide and is bordered by selvages ~17 cm thick. Here, the vein thickness expected for local derivation (~15 cm) is much less than observed; the ratio of externally to internally derived silica is about 62:38. It is highly unlikely that the wallrock schists beyond the selvage margins in the three traverses lost any significant silica, because their mean SiO_2 content of 60.35 ± 2.36 wt% (2σ; Table 1) is statistically identical to that of low-grade, unveined chlorite and biotite zone samples from the Wepawaug (59.81 ± 1.60 wt%; Appendix D in Ague 1994a).

The results show that both veins were conduits for fluid infiltration. The 20% external silica proportion for site 114 is similar to the ~30% average estimated by Ague (1994b). The ~60% external estimate for site 165 is, however, considerably larger; consequently, this vein must have been a major fluid conduit.

Local silica transport from selvages to veins probably occurred by diffusion through a fluid-filled pore network, in which the pores were interconnected, at least transiently. The necessary chemical potential gradients could have arisen due to, for exam-
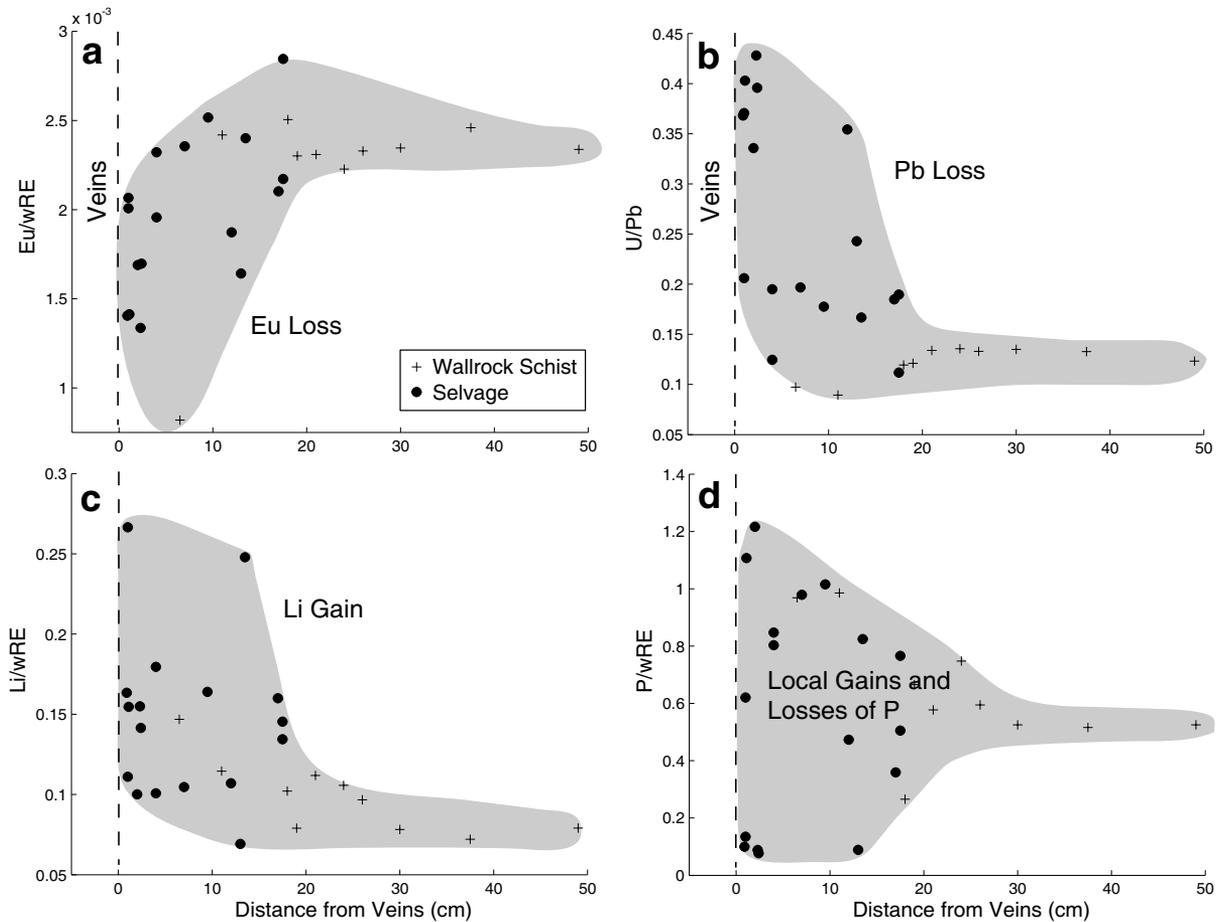
FIGURE 9. Geochemical profiles. Data for all three traverses plotted on the same *x*-axis. (**a**) Eu/*wRE*. Decrease in Eu concentration relative to *wRE* reference frame indicates mass loss. (**b**) U/Pb. U was essentially immobile but Pb was lost, resulting in increases in U/Pb toward veins. (**c**) Li/*wRE*. (**d**) P/*wRE*.

ple, gradients in pressure, fluid composition, surface free energy, or strain energy (e.g., Yardley 1975, 1986; Ramsay 1980; Fisher and Brantley 1992; Ague 2003b; Penniston-Dorland and Ferry 2008). Diffusion down pressure and fluid composition gradients is widely hypothesized but, as discussed by Yardley (1975, 1986), the roles of strain and surface energy could also be important. For example, if matrix quartz grains are highly strained, but crystals in the veins are not, then chemical potential gradients will be set up that act to drive silica to the veins (the strained matrix grains will have higher solubilities). Quantification of strain energy contributions remains as a formidable research challenge.

The impact of surface energy has likewise proven difficult to evaluate. However, in a study of diagenesis in sandstones, Emmanuel et al. (2010) concluded that the solubility of quartz in fine pores (< ~10 um) was significantly larger than in coarser pores as a result of surface energy effects. For metamorphic veins, it is certainly conceivable that the matrix would be dominated by fine-scale pores and the fractures by much larger ones. For such cases, silica might diffuse toward the fractures, leading to depletions in the adjacent selvages. Surface energy may be significant in diagenetic systems, but future work needs to establish whether or not it is important during metamorphism and vein formation.

Mass transfer and mineralogy

The chemical changes due to mass transfer in the selvages must be coupled to changes in modal mineralogy. Modes for a representative selvage and wallrock schist are given in Table 3. To facilitate comparison, the selvage mode is also shown normalized to the same quartz proportion as the wallrock schist. This accounts for any increases in the mode of a mineral due simply to quartz loss to veins during selvage formation.

Reaction progress analysis accounting for mass and volume changes shows that major element mass transfer in the selvages was important for stabilizing aluminous index minerals including staurolite and kyanite; in some cases, increased garnet growth resulted as well (Ague 1994b). Once these minerals began to grow, they were able to incorporate trace elements from infiltrating fluids. Consequently, major and trace element metasomatism were linked.

The selvages gained Mn, HREE, and Y (Figs. 6–8). The Mn mass changes are due to garnet growth during mass transfer, as garnet strongly sequesters Mn. Garnet is far more abundant in the selvages than in wallrock schists; the percentage increase in garnet mode is ~360% when quartz loss is accounted for (Table 3). Mass gains of Y and HREE are also probably related to garnet growth, since metapelitic garnets contain these elements

(Hickmott et al. 1987). Preferential uptake of Sm relative to the lighter REE Nd by garnet can explain the increase in Sm/Nd toward veins (Fig. 8e). In addition, it is possible that dissolution and precipitation of phosphate minerals during selvage formation accounts for some fraction of the HREE and Y uptake (Fig. 9d). The coupling of REE and Y gains suggests REE transport by Y complexes, as hypothesized for the metacarbonate rocks of the Wepawaug (Ague 2003a).

The gains of Fe, Al, Zn, and Li can also be explained by porphyroblast growth. Iron and Al would be concentrated in selvage garnet, staurolite and, in the case of Al, kyanite. Like garnet, the abundance of kyanite increases dramatically in the selvages. The example in Table 3 indicates an increase of over 600%. The mass gains of Al in the selvages demonstrate that there was no net transfer of Al out of them to form vein kyanite. Instead, the infiltrating fluids must have been relatively rich in Al, such that vein kyanite was precipitated and Al was transferred into the selvages. Staurolite is more abundant in selvages as well. Staurolite can contain nontrivial amounts of Zn (Griffen and Ribbe 1973) and Li (Dutrow et al. 1986; Wunder et al. 2007). Thus, incorporation of these elements into staurolite almost certainly accounts for the observed Zn and Li mass gains.

The significant losses of K, Ba, Na, Sr, Eu, Pb, and volatiles are tied to micas and plagioclase. Muscovite and, in some cases, biotite were destroyed in the selvages, accounting for the losses of K, Ba, and volatiles (Fig. 6). In fact, for the example modes in Table 3, prograde muscovite was completely destroyed in the selvage rock. Given that the ionic radii of Pb^{2+} and K^+ are very similar, it is likely that micas were important hosts of Pb, and that mica breakdown facilitated most of the Pb loss from selvages. In addition, muscovite breakdown could have resulted in Sn loss, as this phase can host considerable Sn (Smeds 1992). The losses of Na, Sr, and Eu correspond mostly to the removal of plagioclase feldspar; muscovite breakdown would have also released Na. The modal percentage change for plagioclase in Table 3 is −19% (accounting for quartz loss), but it is observed to be even larger in many other examples. Plagioclase destruction could have also contributed to the Pb loss, but the plagioclase Pb contents would need to be measured to test this possibility. The removal of plagioclase (oligoclase-andesine in these rocks) would be expected to result in Ca loss. However, Ca was taken up by growing garnets so it was not lost. In fact, Ca/wRE may increase adjacent to veins consistent with Ca gain, although there is considerable scatter in the data (not illustrated).

The mass transfer was a metamorphic phenomenon. For example, the gains of Mn, Zn, Li, and Fe demonstrate that mass

transfer occurred during metamorphism, because these elements were taken up by growing garnet and/or staurolite porphyroblasts. Furthermore, the loss of volatiles establishes that veining and selvage formation took place on the prograde path. These conclusions are consistent with the textural evidence that much of the veining occurred after garnets began to grow and continued during amphibolite facies metamorphism (Ague 1994b). For the veins studied herein, a considerable amount of the mass transfer must have occurred at peak kyanite zone conditions, as the veins contain kyanite (Figs. 2 and 3).

Previous study of selvages around two other examples of veins cutting staurolite-kyanite zone rocks of the Wepawaug found gains of Fe, Mn, and Zn, as well as losses of Si, K, Na, Ba, Sr, and volatiles in one or both examples, similar to the results herein (Ague 1994b). Some minor differences, including losses of Rb and, in one example, Ca are also apparent. The most notable differences are that the veins of the earlier study lack kyanite, and that there was no discernable net Al mass transfer to or from selvages. In the Wepawaug Schist, therefore, the presence of vein kyanite is probably a good indication that external fluid fluxes were sufficient to transport and deposit considerable Al, in contrast to those vein systems that lack kyanite. As a consequence, the strongly peraluminous nature of the selvages around kyanite-bearing veins of this study results from both alkali metal losses and Al gains (Figs. 8c and 9d). The mass transfer of Al and other constituents must have taken place in the presence of a fluid phase, as transport rates in fluid-undersaturated and anhydrous systems are prohibitively slow (Carlson 2010). Comparisons for Y, REE, Pb, Sn, and Li are not possible as the compositional data are not available in Ague (1994b).

Sodium mass transfer and infiltration history

Sodium was lost in an average sense from the selvages due to plagioclase and muscovite breakdown, but the Na/wRE profiles for the individual traverses indicate complex geochemical behavior (Fig. 10). Sodium is depleted in the selvages for each profile relative to wallrock schists. However, Na rises sharply and peaks at the transition between the silica-depleted selvage regions and the less altered wallrock schists. Sr/wRE profiles are similar (not shown). Mineralogically, the Na (and Sr) peaks are due to large amounts of modal plagioclase. The fact that these peaks are found precisely at the boundary of the silica-depleted region in all three traverses strongly suggests that they are metasomatic phenomena, not random compositional heterogeneity inherited from the original sediments.

It is much less clear, however, what process or processes produced the peaks. One possibility is that geochemical self-organization during diffusion-dominated mass transfer and reaction produced a plagioclase-rich reaction zone (e.g., Thompson 1959; Brady 1977; Brimhall 1977). Another is a multi-stage infiltration-reaction scenario. First, Na (and Sr) were added to the rock by vein fluids. Sodium transport as alkali-Al-Si complexes (cf. Manning 2007; Wohlers and Manning 2007, 2009) could have produced early plagioclase enrichment in the selvage margins, as well as explain the presence of sodic plagioclase in some Wepawaug veins (e.g., site 165). Later, the fluid composition must have changed such that plagioclase became unstable, thus facilitating Na removal from the rock. There is some field

TABLE 3. Mode comparison

	114ii Selvage	114ii Normalized selvage	114vi Wallrock schist	% Mode change 114vi → 114ii Norm
Quartz	11.8	39.9	39.9	–
Muscovite	–	–	24.3	−100
Biotite	33.7	23.0	26.0	−12
Garnet	16.3	11.1	2.42	360
Kyanite	30.0	20.4	2.80	630
Staurolite	2.54	1.73	–	∞
Plagioclase	4.59	3.13	3.86	−19
Fe-Ti oxides	1.07	0.73	0.72	1

Note: Mineral modes for 114ii Normalized selvage adjusted using wallrock schist value of 39.9 vol% quartz.

evidence for such a change, as kyanite replaces plagioclase in the site 165 vein (Fig. 3d; vein plagioclase is absent at site 114). In this multi-stage scenario, the observed plagioclase-rich zones would be remnants of once thicker plagioclase-rich selvages.

The scatter in the data for the combined geochemical profiles makes it difficult to quantify the respective roles of diffusion, mechanical dispersion, and advection during reactive transport (Figs. 7–10). All of these processes likely operated, and their nature and intensity varied during the course of vein formation.

Simple model of strongly channelized flow

It has long been known that fractures and other regions of increased permeability can strongly channelize fluid flow (e.g., Baker 1955; Huitt 1956; Snow 1969; Neuzil and Tracy 1981; Long et al. 1982). A simple two-dimensional numerical model of upward, steady-state fluid flow through a porous medium was constructed to investigate how fluid fluxes may vary in and around veins. The model flow region is 10×10 m—appropriate for visualizing outcrop-scale flux heterogeneities (Fig. 11). It contains four randomly positioned, high-permeability zones (model fractures) that are 0.25 m wide and 0.5 to 3.5 m long. The background rock matrix permeability in both directions and the horizontal component of the fracture permeability are 10^{-20} m^2. The vertical component of the fracture permeability is

two orders of magnitude greater (10^{-18} m^2). No flow is allowed across the left and right boundaries of the flow region. The initial fluid pressure gradient from which the steady state developed was lithostatic across the flow region, and fluid pressure remains fixed at the upper and lower boundaries. The governing equations and solution procedures are identical to those used by Ague (2007); the reader is referred to this paper for more detailed discussion. The spatial distribution of flux highs and lows in the model depends almost entirely on the permeability *contrast* between fractures and matrix, not the absolute permeability values. Consequently, fluxes are shown normalized to the maximum value for ease of interpretation. Vein spacings in outcrop are typically at the decimeter to meter scale; the model veins are spaced more widely simply for graphical clarity.

The model predicts extremely steep fluid flux gradients around the model vein fracture conduits, consistent with earlier models of channelized flow (Fig. 11; e.g., Breeding et al. 2004). Flux magnitude in fractures scales with fracture length, such that the largest fluxes are developed in fractures greater than ~2 m long. Flow is strongly focused into the high permeability zones, leaving the directly adjacent areas impoverished in fluid, as shown for the points labeled *b* in Figure 11b. The "background" fluxes in the regions distal to veins, such as point *c*, are also very small relative to the fractures (Fig. 11b). The high-flux margins
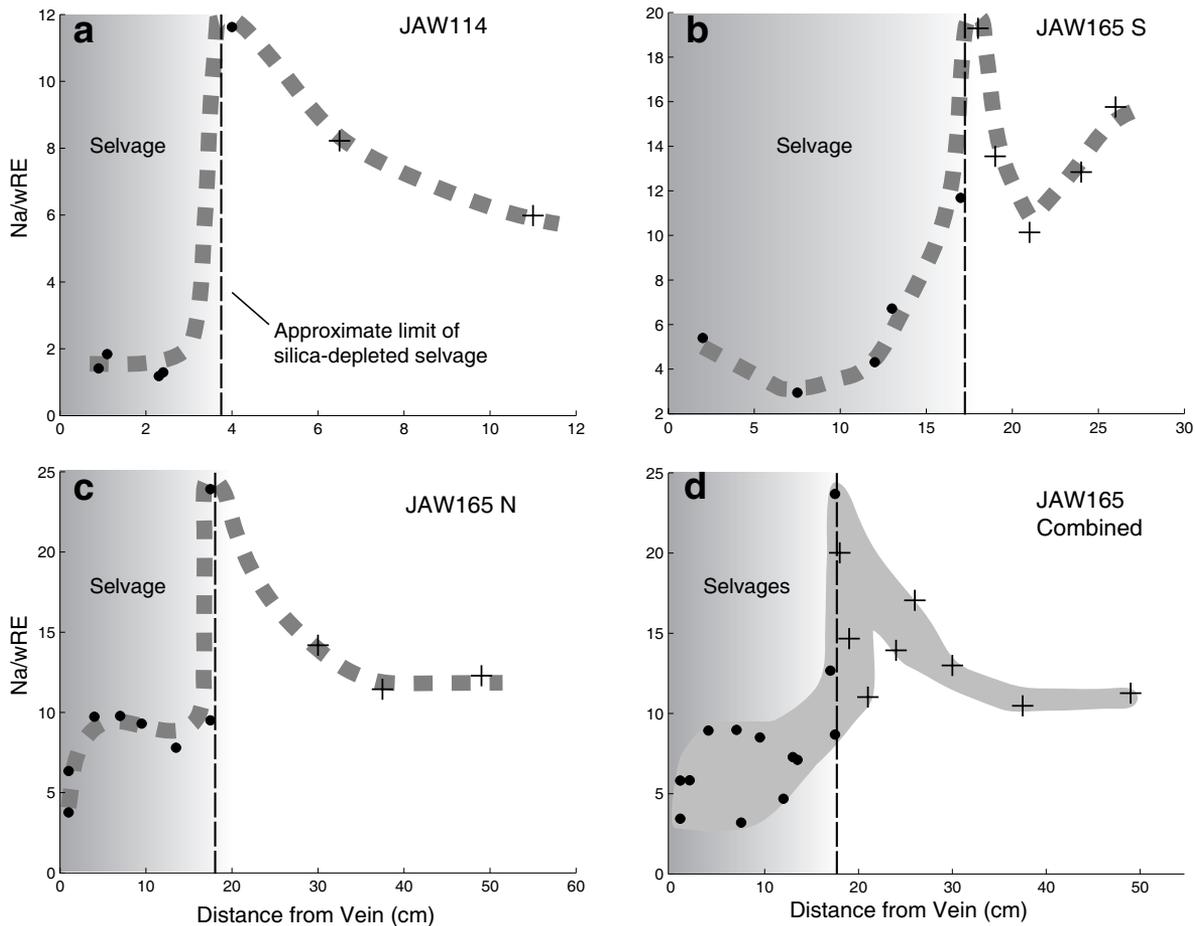
FIGURE 10. Geochemical profiles for Na/*wRE*. Note peak in Na contents at approximate limits of silica-depleted selvages (vertical dashed lines). (**a**) Site 114. (**b**) Site 165 (south). (**c**) Site 165 (north). (**d**) Site 165, south and north combined.

of the fracture conduits are analogs for contacts between veins and selvages (e.g., point *a*, Fig. 11b). Note, however, that fluxes are predicted to drop off rapidly into the selvages and out into the wallrock schists. Fluxes in the lowest-flow areas like point *b* can be nearly two orders of magnitude less than those within the model veins (Figs. 11b and 12). The flux difference between the conduits and the adjacent low-flow areas would be even greater if conduit-matrix permeability contrasts were larger.

Inflow and outflow areas are predicted to develop at the tips of cracks. This flow could give rise to distinctive metasomatic phenomena. Given that these inflow/outflow areas are fairly small relative to the length of the fractures, it is likely that regions around the midsections of fractures were sampled in this study (e.g., points *a*, *b*). Investigation of fracture tips is an important target for future work.

Diffusion will transport mass along the flow direction and perpendicular (or at some high angle) to it. Although advective fluxes in the areas immediately adjacent to veins may be small, diffusion will still be significant as long as a pore fluid is present (Fig. 12). The shapes of many of the profiles, such as Mn/*wRE* (Fig. 7e), are qualitatively consistent with diffusional transport into or out of selvages during reaction, at least for some part of the infiltration history. Such chemical (or isotopic) gradients will be preserved for species with small volumetric fluid/rock partition coefficients (Fig. 12; Bickle 1992). On the other hand, larger alteration halos would be expected for $^{18}O/^{16}O$ owing to the large fluid/rock partition coefficient for oxygen (Bickle 1992; Palin 1992). Such alteration could even span the distance between veins if transport-reaction was of sufficient duration, particularly if veins are closely spaced. Length scales of diffusional transport and reaction for CO_2 could likewise be large (Ague 2003a, 2003b; Penniston-Dorland and Ferry 2006). For these cases of large alteration distances, chemical or isotopic gradients from selvages across wallrocks could be small to negligible. This is in contrast to the species behavior illustrated in Figures 7–10, which is characterized by strong local gradients.

The model selvages have low permeability. Consequently, they undergo little fluid flow. It is possible that processes such as mineral dissolution or fracturing could occur in the selvages, thus increasing their porosity and permeability. In these cases, fluid flow through the selvages could become an important part of the overall mass transfer.

Of course, long-term fluid flow in deforming metamorphic rocks will be far more complex than in the model. Cracks may form by a variety of time-dependent processes, including hydrofracturing and tectonic deformation. Veins are commonly built up via repeated fracturing and sealing events (Ramsay 1980; Ague 1994b). Flow is likely to be transient because once the fractures open, mineral precipitation and collapse of the surrounding wallrock will act to seal them. However, because hydrous fluids are relatively incompressible at high pressures, near steady-state flow patterns could evolve rapidly (day to week timescales for the model in Fig. 11). Consequently, channelized flow similar to Figure 11 could develop even over the potentially brief lifetimes of fracture opening and closing events.

Despite the model simplifications, the results demonstrate that order-of-magnitude flux contrasts over relatively short length scales are to be expected in rocks that contain high-permeability

conduits. This would be true even if the flow depicted in Figure 11 was part of a local convective system of the type suggested by Yardley (1986). Furthermore, pulsed flow of fluid through upwardly migrating conduits (e.g., Yardley 1986; Connolly and Podladchikov 2007) or chanellization due to a reactive dissolution process (e.g., Spiegelman and Kelemen 2003) would also be expected to generate steep local flux gradients around conduits. The observed steep gradients in metasomatic intensity around
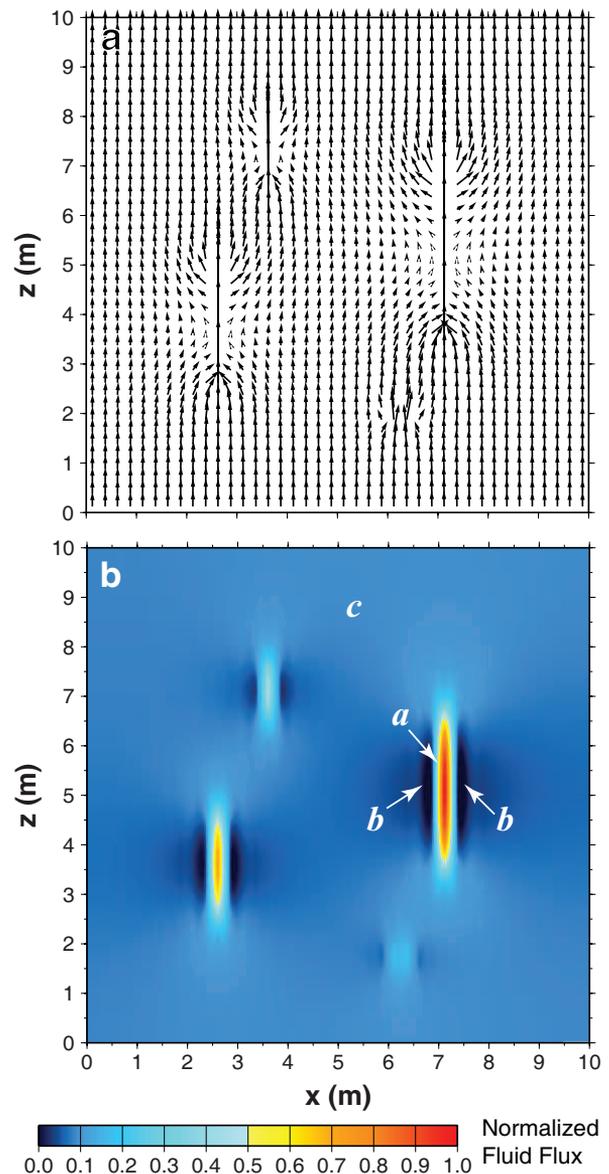
FIGURE 11. Simple two-dimensional models of upward fluid flow. (**a**) Vectors illustrating magnitude and direction of fluid flow; vector length scales with flux magnitude. Note focusing of flow into four high permeability zones (model fractures) of varying lengths. (**b**) Fluid fluxes normalized to the maximum flux value. Largest fluxes are predicted in the model fractures and directly at fracture-rock contacts (e.g., point *a*). Channelization of fluid into the fractures impoverishes the surroundings in fluid such that the lowest flux areas are found adjacent to the fractures (e.g., points labeled *b*). "Background" fluxes away from fractures are also small (e.g., point *c*).
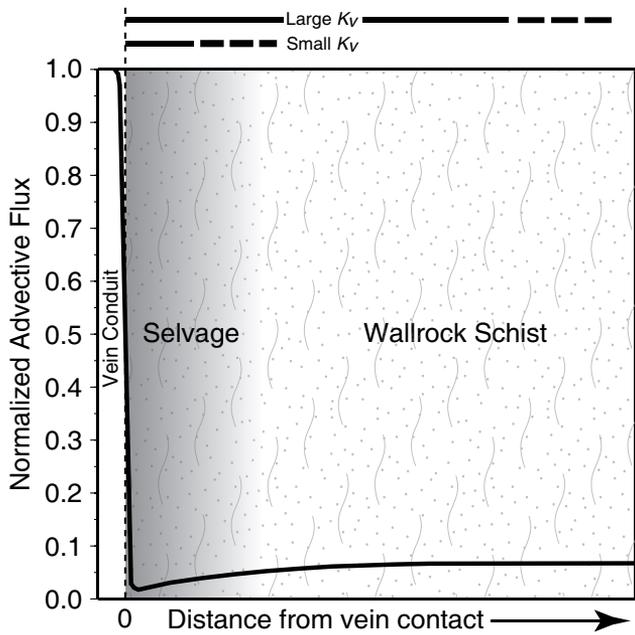
Figure 12. Cartoon of normalized fluid flux vs. distance perpendicular to midsection of large fracture/vein conduit. Flow direction is normal to the x-y axes and the page. Large advective fluxes are predicted for the high-permeability conduit and the contact between the conduit and the adjacent selvage (vertical dashed line). Mass transfer, largely by diffusion at the centimeter to decimeter scale perpendicular to the conduit, causes metasomatic alteration of rock. This occurs mostly within the selvage for elements with small volumetric fluid-rock partition coefficients (K_v) such as Mn (characteristic distance shown with thick horizontal line). Tracers with larger K_v, such as $^{18}O/^{16}O$, will have larger alteration halos.

veins are fully consistent with the predicted steep flux gradients around fractures (Fig. 11).

CONCLUDING REMARKS

The formation of quartz-kyanite veins during Barrovian metamorphism of the Wepawaug Schist produced changes in rock chemistry that were strongly coupled to mineralogical changes. Extensive porphyroblast growth in selvages adjacent to the veins resulted in the uptake of: (1) Fe, Mn, HREE, and Y by garnet; (2) Fe, Zn, and Li by staurolite, and (3) Al by kyanite, staurolite, and garnet. Through-going, external fluids flowing along fractures (veins) transported the elements into the rocks. Infiltration into the adjacent selvages by diffusion with some contribution from fluid flow supplied these elements to the growing porphyroblasts. Interestingly, Li is typically lost during prograde devolatilization (Teng et al. 2007). The results presented herein show, however, that if a phase with a strong preference for Li like staurolite is crystallizing, then the Li can be scavenged from infiltrating fluids yielding overall Li mass gains.

Elements were also lost from the selvages. Widespread breakdown of micas (particularly muscovite) led to losses of K, Na, Ba, Pb, Sn, and volatiles, whereas plagioclase breakdown liberated Na, Sr, and Eu. Silica losses were very large, averaging 50%. The bulk of this silica was transferred locally to the adjacent veins. However, mass balance analysis shows that all of the vein silica could not have been supplied locally from the selvages; between 20 and 60% had to be precipitated from external fluids.

This important component of externally derived quartz is consistent with earlier results for Barrovian metamorphism in New England (Ague 1994b; Penniston-Dorland and Ferry 2008). For example, Penniston-Dorland and Ferry (2008) concluded that over 90% of the silica in quartz veins of the Waits River Formation, Vermont, was derived externally. As shown in these earlier studies, the time-integrated fluid fluxes (q_{TI}) necessary to precipitate such volumes of external quartz at the outcrop scale are enormous [$2–6 \times 10^4$ m$^3_{(Fluid)}$ m$^{-2}_{(Rock)}$; Ague 1994b, 2003a; Penniston-Dorland and Ferry 2008]. As typical regional q_{TI} values in collisional orogens will be roughly one order of magnitude smaller than this (Lyubetskaya and Ague 2009), the large fluxes recorded by the veins require major focusing of fluids into conduits at the outcrop scale or larger. The large fluid fluxes may have been able to transport heat (Ferry 1992; Ague 1994b).

Interestingly, despite the high q_{TI} values, the kyanite zone selvages investigated by Penniston-Dorland and Ferry (2008) are noticeably thinner than those investigated here, and they underwent less (although still considerable) metasomatic alteration. Chemical fluid-rock exchanges between veins and selvages were evidently less extensive in the Waits River than in the Wepawaug, perhaps due to lower wallrock porosity or permeability; somewhat lower pressures of metamorphism; differences in lithology (some of the Waits River examples are carbonate bearing); or differences in the source(s), length scales, and timing of fluid flow.

In the Wepawaug Schist, the large fluid fluxes transported significant Al. The kyanite that grew in the veins was not derived via Al loss from adjacent selvages, because the selvages actually gained Al. This result is comparable to that of Bucholz and Ague (2010), who documented evidence for Al addition in and around the classical Barrovian quartz-kyanite veins studied by Read (1932) on Unst, Shetland Islands, Scotland. The Unst selvages are silica-depleted and lost Na, K, Ba, Sr, and volatiles due to the breakdown of muscovite and paragonite; the suite of elements that was lost is similar to that for the Wepawaug Schist.

The Wepawaug Schist and Unst results are, however, different from the metasomatism recorded at several other localities, including the veins and selvages cutting chlorite through staurolite zone rocks in the northeastern part of the Barrovian sequence, Scotland (Masters and Ague 2005). Here, instead of Na loss, Na, Ca, and related elements like Sr were gained due mostly to plagioclase growth, whereas K, Rb, and Ba were lost as a result of mica (primarily muscovite) destruction. The process can be modeled largely as Na-Ca-K exchange between rocks and infiltrating Cl-bearing aqueous fluids. In the Otago Schist, New Zealand, Breeding and Ague (2002) described metasomatic effects that are broadly comparable, although here the mass transfer is most extensive in the higher-grade rocks of the sequence (greenschist facies). Sodium and most likely Ca were gained, whereas K was lost. Furthermore, quartz precipitation in veins added silica to the higher-grade outcrops. Dasgupta et al. (2009) also described Na+Ca gains, K losses, and silica addition during Barrovian metamorphism in Sikkim Himalaya. However, the magnitude of the mass transfer as well as the growth of quartz veins were apparently more limited than in the northeastern Barrovian, the

Otago Schist, the Wepawaug Schist, or the schists of Unst.

The issue of why Na was gained and K was lost at some localities (e.g., northeastern Barrovian), whereas both were lost at others (e.g., Wepawaug, Unst) remains as a significant problem. The role of pressure may turn out to be particularly important in this regard. Pressures at peak temperatures were quite high for the Wepawaug Schist (0.8–1.0 GPa) and the Unst metapelites (>1.0 GPa). It could be that at these higher pressures, the coupled mass transfer of K-Na-Al-Si was accomplished by polymerization and fluid transport as neutral complexes instead of Cl species, consistent with a growing body of high-pressure experimental work (Manning 2006, 2007).

I hypothesize that disagreement in the literature regarding the nature and extent of element mobility during Barrovian metamorphism stem largely from the extremely channelized nature of fracture-controlled flow. Extensive chemical alteration driven by fluid infiltration is not pervasive throughout the rock mass, but is instead concentrated in centimeter- to decimeter-wide selvages bordering the fractures. As a consequence, conclusions reached regarding the presence or absence of significant metasomatism will depend strongly on sample locations. A study based on selvages would document extensive mass transfer. On the other hand, a sampling focus on areas such as point *c* in Figure 11b would discover little or perhaps no elemental mass transfer, as fluxes in these areas would generally have been too small to modify the compositions of rocks unless gradients in fluid compositions were very large. Furthermore, the intensity of selvage metasomatism will vary from region to region based on as yet incompletely understood factors relating to pressure–temperature regimes, fluid sources and flow paths, and the geochemical, lithologic, and tectonic environments of flow. Considerable non-volatile element mass transfer could also develop in and around other kinds of conduits such as high-permeability lithologic contacts; this has been demonstrated, for example, in the metacarbonate rocks of the Wepawaug Schist (Hewitt 1973; Tracy et al. 1983; Palin 1992; Ague 2003a) and many other localities worldwide.

Importantly, however, not all geochemical alteration effects will be localized in and around selvages. As discussed above, alteration halos for oxygen isotope ratios may extend beyond selvage margins well into surrounding wallrock schists due to the large fluid/rock partition coefficient for oxygen (Fig. 12). If the isotopic metasomatism spans the distance between veins, then the intervening wallrock will be largely equilibrated with the vein fluids and oxygen isotope "selvages" will be absent. Consequently, an oxygen isotope study of unzoned minerals such as quartz may not record the fluid infiltration that occurred. On the other hand, complete equilibration is unlikely, as refractory minerals such as garnet can preserve isotopic zoning and thus record changes in wallrock composition if the crystals grow during infiltration (e.g., Page et al. 2010). As a result, the isotopic signals preserved in refractory zoned porphyroblasts have great potential to reveal fluid infiltration histories, even in cases where other matrix minerals have largely equilibrated with vein fluids; van Haren et al. (1996) present an example from the Wepawaug Schist. Furthermore, the ion microprobe now allows quantification of oxygen isotopic zoning patterns at unprecedented spatial resolution, and can resolve very fine-scale features related to infiltration even for minerals like quartz and calcite that have relatively fast rates of intracrystalline diffusion (cf. Valley and Kita 2009). Oxygen isotope studies of bulk quartz from veins and wallrocks that neglect zonation in porphyroblasts and other phases may come to erroneous conclusions regarding fluid infiltration.

The presence of both steep and broad gradients in metasomatic intensity poses formidable challenges to field studies. For example, protolith heterogeneities as well as extreme spatial variations in the extent of elemental mass transfer can swamp the chemical signal of metasomatism, unless many samples and statistical techniques appropriate for compositional data are used (van Haren and Ague 1996). Although the selvages generally have centimeter- to decimeter-scale widths, one cannot jump to the conclusion that fracture-related mass transfer is restricted to these scales. Indeed, the fluid flow *along* the fractures was a major part of the regional metamorphic hydrology, as evidenced by the fact that the veins record enormous time-integrated fluid fluxes.

Yardley (2009) asserts that examples of metasomatic alteration of wallrocks by vein fluids are rare (e.g., his Fig. 10). However, quantitative mass balance studies of vein–selvage–wallrock systems are also relatively rare. Consequently, in my opinion, much remains to be learned before the full impact of veining on metamorphic mass transfer can be rigorously assessed. Despite the relatively small database, existing work shows that significant mass transfer in and around veins occurred during Barrovian-style metamorphism in parts of several important regional metamorphic belts, including the Scottish Dalradian and the New England Appalachians.

Ultimately, an important goal for future field-based work is to effectively integrate flux and mass transfer results from the outcrop scale to the regional scale. In a larger sense, fractured metamorphic systems may contribute to geochemical cycling by acting as giant sources or sinks of elements, including elements of economic significance. The metamorphic fluids of the Wepawaug Schist would have become progressively depleted in Mn, Zn, Li, and HREE but enriched in Sn and Pb along their deep-crustal, amphibolite facies flow paths.

ACKNOWLEDGMENTS

REFERENCES CITED

Ague, J.J. (1994a) Mass transfer during Barrovian metamorphism of pelites, south-central Connecticut, I: Evidence for composition and volume change. American Journal of Science, 294, 989–1057.
——— (1994b) Mass transfer during Barrovian metamorphism of pelites, south-central Connecticut, II: Channelized fluid flow and the growth of staurolite and kyanite. American Journal of Science, 294, 1061–1134.
——— (1995) Mass transfer during Barrovian Metamorphism of Pelites, south-central Connecticut—Reply. American Journal of Science, 295, 1025–1033.
——— (1997) Compositional variations in metamorphosed sediments of the Littleton Formation. American Journal of Science, 297, 440–449.
——— (2003a) Fluid infiltration and transport or major, minor, and trace elements during regional metamorphism of carbonate rocks, Wepawaug Schist, Connecticut, USA. American Journal of Science, 303, 753–816.

———(2003b) Fluid Flow in the Deep Crust. In R.L. Rudnick, Ed., H.D. Holland and K.K. Turekian, Executive Eds., Treatise on Geochemistry, volume 3, The Crust, p. 195–228. Elsevier, Oxford.

——— (2007) Models of permeability contrasts in subduction zone mélange: Implications for gradients in fluid fluxes, Syros and Tinos Islands, Greece. Chemical Geology, 239, 217–227.

Ague, J.J. and van Haren, J.L.M. (1996) Assessing metasomatic mass and volume changes using the bootstrap, with application to deep-crustal hydrothermal alteration of marble. Economic Geology, 91, 1169–1182.

Aitchison, J. (1986) The statistical analysis of compositional data. Chapman and Hall, London, 416 p.

Baker, W.J. (1955) Flow in Fissured Formations. Proceedings of the 4th World Petroleum Congress, section II/E, p. 379–393, Carlo Columbo Publishers, Rome.

Baumgartner, L.P., and Olsen, S.N. (1995) A least-squares approach to mass transport calculations using the isocon method. Economic Geology, 90, 1261–1270.

Bebout, G.E. and Barton, M.D. (1989) Fluid flow and metasomatism in a subduction zone hydrothermal system: Catalina Schist terrane, California. Geology, 17, 976–980.

Beinlich, A., Klemd, R., John, T., and Gao, J. (2010) Trace-element mobilization during Ca-metasomatism along a major fluid conduit: Eclogitization of blueschist as a consequence of fluid–rock interaction. Geochimica et Cosmochimica Acta, 74, 1892–1922.

Beitter, T., Wagner, T., and Markl, G. (2008) Formation of kyanite-quartz veins of the Alpe Sponda, Central Alps Switzerland: implications for Al transport during regional metamorphism. Contributions to Mineralogy and Petrology, 156, 689–707.

Bickle, M.J. (1992) Transport mechanisms by fluid flow in metamorphic rocks: Oxygen and strontium decoupling in the Trois Seigneurs Massif – a consequence of kinetic dispersion? American Journal of Science, 292, 289–316.

Brady, J.B. (1977) Metasomatic zones in metamorphic rocks. Geochimica et Cosmochimica Acta, 41, 113–125.

Breeding, C.M. and Ague, J.J. (2002) Large-scale flow of slab-derived fluids in an accretionary prism, Otago Schist, New Zealand. Geology, 30, 499–502.

Breeding, C.M., Ague, J.J., Bröcker, M., and Bolton, E.W. (2003) Blueschist preservation in a retrograded, high-pressure, low-temperature metamorphic terrane, Tinos, Greece: Implications for fluid flow paths in subduction zones. Geochemistry, Geophysics, and Geosystems, 4, 9002, doi:10.1029/2002GC000380, 11 p.

Brimhall, G.H., Jr. (1977) Early fracture-controlled disseminated mineralization at Butte. Economic Geology, 72, 37–59.

Brimhall, G.H., Lewis, C.J., Ague, J.J., Dietrich, W.E., Hampel, J., Teague, T., and Rix, P. (1988) Metal enrichment in bauxites by deposition of chemically mature aeolian dust. Nature, 333, 819–824.

Bucholz, C.E. and Ague, J.J. (2010) Fluid flow and Al transport during quartz-kyanite vein formation, Unst, Shetland Islands, Scotland. Journal of Metamorphic Geology, 28, 19–39.

Carlson, W.D. (2010) Dependence of reaction kinetics on H_2O activity as inferred from rates of intergranular diffusion of aluminum. Journal of Metamorphic Geology, 28, 735–752.

Connolly, J.A.D. and Podladchikov, Y.Y. (2007) Decompaction weakening and channeling instability in ductile porous media: Implications for asthenospheric melt segregation. Journal of Geophysical Research, 112, B10205, doi:10.1029/2005JB004213.

Dasgupta, S., Chakraborty, S., and Neogi, S. (2009) Petrology of an inverted Barrovian sequence of metapelites in Sikkim Himalaya, India: Constraints on the tectonics of inversion. American Journal of Science, 309, 43–84.

Dipple, G.M., Wintsch, R.P., and Andrews, M.S. (1990) Identification of the scales of differential element mobility in a ductile fault zone. Journal of Metamorphic Geology, 8, 645–661.

Dipple, G.M. and Ferry, J.M. (1992) Metasomatism and fluid flow in ductile fault zones. Contributions to Mineralogy and Petrology, 112, 149–164.

Durand, C., Marquer, D., Baumgartner, L.P., Goncalves, P., Boulvais, P., and Rossy, M. (2009) Large calcite and bulk-rock volume loss in metacarbonate xenoliths from the Quérigut massif (French Pyrenees). Contributions to Mineralogy and Petrology, 157, 749–763.

Dutrow, B.L., Holdaway, M.J., and Hinton, R.W. (1986) Lithium in staurolite and its petrologic significance. Contributions to Mineralogy and Petrology, 94, 496–506.

Evans, B.W. (2007) Barrovian metamorphism. In B.W. Evans, Ed. and B.J Wood, Executive Ed., Landmark Papers: Metamorphic Petrology, p. L9–L14. Mineralogical Society of Great Britain and Ireland.

Emmanuel, S., Ague, J.J., and Walderhaug, O. (2010) Evolution of pore size distributions during quartz precipitation in sandstone and the impact of interfacial energy on reaction kinetics. Geochimica et Cosmochimica Acta, 74, 3539–3552.

Ferry, J.M. (1987) Metamorphic hydrology at 13-km depth and 400–500 °C. American Mineralogist, 72, 39–58.

——— (1992) Regional Metamorphism of the Waits River Formation, eastern Vermont, Delineation of a new type of giant metamorphic hydrothermal system. Journal of Petrology, 33, 45–94.

Fisher, D.M. and Brantley, S.L. (1992) Models of quartz overgrowth and vein formation: Deformation and episodic fluid flow in an ancient subduction zone. Journal of Geophysical Research, 97, 20042–20061.

Franz, L., Romer, R.L., Klemd, R., Schmid, R., Oberhänsli, R., Wagner, T., and Schuwen, D. (2001) Eclogite–facies quartz veins within metabasites of the Dabie Shan (eastern China): pressure–temperature–time–deformation path, composition of the fluid phase and fluid flow during exhumation of high-pressure rocks. Contributions to Mineralogy Petrology, 141, 322–346.

Fritts, C.E. (1962) Age and sequence of metasedimentary and metavolcanic formations northwest of New Haven, Connecticut. United States Geological Survey Professional Paper, 450-D, D32–D36.

——— (1963) Bedrock geology of the Mount Carmel quadrangle, Connecticut. U.S. Geological Survey Quadrangle Map, GQ-199.

———(1965a) Bedrock geologic map of the Ansonia quadrangle, Fairfield and New Haven Counties, Connecticut. U.S. Geological Survey Quadrangle Map, GQ-426.

———(1965b) Bedrock geologic map of the Milford quadrangle, Fairfield and New Haven Counties, Connecticut. U.S. Geological Survey Quadrangle Map, GQ-427.

Gao, J., John, T., Klemd, R., and Xiong, X. (2007) Mobilization of Ti–Nb–Ta during subduction: evidence from rutile-bearing dehydration segregations and veins hosted in eclogite, Tianshan, NW China. Geochimica et Cosmochimica Acta, 71, 4974–4996.

Grant, J.A. (1986) The isocon diagram – a simple solution to Gresens' equation for metasomatic alteration. Economic Geology, 81, 1976–1982.

Gresens, R.L. (1967) Composition-volume relations of metasomatism. Chemical Geology, 2, 47–65.

Griffen, D.T. and Ribbe, P.H. (1973) The crystal chemistry of staurolite. American Journal of Science, 273-A, 479–495.

Harlov, D.E., Hansen, E.C., and Biggler, C. (1998) Petrologic evidence for K-feldspar metasomatism in granulite facies rocks. Chemical Geology, 151, 373–386.

Hewitt, D.A. (1973) The metamorphism of micaceous limestones from south-central Connecticut. American Journal of Science, 273-A, 444–469.

Hibbard, J.P., van Staal, C.R., and Rankin, D.W. (2007) A comparative analysis of pre-Silurian crustal building blocks of the northern and southern Appalachian orogen. American Journal of Science, 307, 23–45.

Hickmott, D.D., Shimizu, N., Spear, F.S., and Selverstone, J. (1987) Trace element zoning in a metamorphic garnet. Geology, 15, 573–576.

Huitt, J.L. (1956) Fluid flow in simulated fractures. American Institute of Chemical Engineers Journal, 2, 259–264.

Jiang, S., Wang, R., Xu, X., and Zhao, K. (2005) Mobility of high field strength elements HFSE in magmatic-, metamorphic-, and submarine-hydrothermal systems. Physics and Chemistry of the Earth, 30, 1020–1029.

Johnson, M.C. and Plank, T. (1999) Dehydration and melting experiments constrain the fate of subducted sediments. Geochemistry, Geophysics, Geosystems, 1, 1999GC000014.

Lancaster, P.J., Baxter, E.F., Ague, J.J., Breeding, C.M., and Owens, T.L. (2008) Synchronous peak Barrovian metamorphism driven by syn-orogenic magmatism and fluid flow in southern Connecticut, USA. Journal of Metamorphic Geology, 26, 527–538.

Long, J.C.S., Remer, J.S., Wilson, C.R., and Witherspoon, P.A. (1982) Porous media equivalents for networks of discontinuous fractures. Water Resources Research, 18, 645–658.

Lyubetskaya, T. and Ague, J.J. (2009) Modeling the magnitudes and directions of regional metamorphic fluid flow in collisional orogens. Journal of Petrology, 50, 1505–1531.

Manning, C.E. (1997) Coupled reaction and flow in subduction zones: Silica metasomatism in the mantle wedge. In: B. Jamtveit and B.W.D. Yardley Eds., Fluid Flow and Transport in Rocks, p. 139–148. Chapman-Hall, London.

——— (2006) Mobilizing aluminum in crustal and mantle fluid. Journal of Geochemical Exploration, 89, 251–253.

——— (2007) Solubility of corundum + kyanite in H_2O at 700°C and 10 kbar: evidence for Al-Si complexing at high pressure and temperature. Geofluids, 7, 258–269.

Masters, R.L. and Ague, J.J. (2005) Regional-scale fluid flow and element mobility in Barrow's metamorphic zones, Stonehaven, Scotland. Contributions to Mineralogy and Petrology, 150, 1–18.

McLellan, E.L. (1989) Sequential formation of subsolidus and anatectic migmatites in response to thermal evolution, eastern Scotland. Journal of Geology, 97, 165–182.

Meyer, C. (1965) An early potassic type of alteration at Butte, Montana. American Mineralogist, 50, 1717–1722,

Miller, D.P., Marschall, H., and Schumacher, J.C. (2009) Metasomatic formation and petrology of blueschist-facies hybrid rocks from Syros (Greece): Implications for reactions at the slab–mantle interface. Lithos, 107, 53–67.

Moss, B.E., Haskin, L.A., and Dymek, R.F. (1996) Compositional variations in metamorphosed sediments of the Littleton Formation, New Hampshire, and the Carrabassett Formation, Maine, at sub-hand specimen, outcrop, and regional scales. American Journal of Science, 296, 473–505.

Nabelek, P. (1997) Quartz-sillimanite leucosomes in high-grade schists, Black Hills, South Dakota: a perspective on the mobility of Al in high-grade metamorphic rocks. Geology, 25, 995–998.

Neuzil, C.E. and Tracy, J.V. (1981) Flow through fractures. Water Resources Research, 17, 191–199.

Newton, R.C. and Manning, C.E. (2000) Quartz solubility in H_2O-NaCl and H_2O-CO_2 solutions at deep crust-upper mantle pressures and temperatures: 2–15 kbar and 500–900 °C. Geochimica et Cosmochimica Acta, 64, 2993–3005.

Oliver, N.H.S. (1996) Review and classification of structural controls on fluid flow during regional metamorphism. Journal of Metamorphic Geology, 14, 477–492.

Oliver, N.H.S., Dipple, G.M., Cartwright, I., and Schiller, J. (1998) Fluid flow and metasomatism in the genesis of the amphibolite-facies, pelite-hosted Kanmantoo copper deposit, South Australia. American Journal of Science, 298, 181–218.

Orville, P.M. (1969) A model for metamorphic differentiation origin of thin-layered amphibolites. American Journal of Science, 267, 64–86.

Page, F.Z., Kita, N.T., and Valley, J.W. (2010) Ion microprobe analysis of oxygen isotopes in garnets of complex chemistry. Chemical Geology, 270, 9–19.

Palin, J.M. (1992) Stable isotope studies of regional metamorphism in the Wepawaug Schist, Connecticut. Ph.D. thesis, 170 p. Yale University, New Haven.

Penniston-Dorland, S.C. and Ferry, J.M. (2006) Development of spatial variations in reaction progress during regional metamorphism of micaceous carbonate rocks, Northern new England. American Journal of Science, 306, 475–524.

——— (2008) Element mobility and scale of mass transport in the formation of quartz veins during regional metamorphism of the Waits River Formation, east-central Vermont. American Mineralogist, 93, 7–21.

Podladchikov, Y.Y., John, T., Beinlich, A., and Klemd, R. (2009) Channeled fluid flow through slabs: reactive porosity waves. American Geophysical Union, Fall Meeting, abstract V13D-2066.

Ramsay, J.G. (1980) The crack-seal mechanism of rock deformation. Nature, 284, 135–139.

Read, H.H. (1932) On quartz-kyanite rocks in Unst, Shetland Islands, and their bearing on metamorphic differentiation. Mineralogical Magazine, 23, 317–328.

Rodgers, J. (1985) Bedrock Geological Map of Connecticut. Connecticut Geological and Natural History Survey, Department of Environmental Protection, scale 1:125,000.

Rye, R.O., Schuiling, R.D., Rye, D.M., and Jansen, J.B.H. (1976) Carbon, hydrogen and oxygen isotope studies of the regional metamorphic complex at Naxos, Greece. Geochimica et Cosmochimica Acta, 40, 1031–1049.

Selverstone, J., Morteani, G., and Staude, J.M. (1991) Fluid channeling during ductile shearing—transformation of granodiorite to aluminous schist in the Tauern Window, Eastern Alps. Journal of Metamorphic Geology, 9, 419–431.

Selverstone, J., Franz, G., Thomas, S., and Getty, S. (1992) Fluid variability in 2 GPa eclogites as an indicator of fluid behavior during subduction. Contributions to Mineralogy and Petrology, 112, 341–357.

Sepahi, A.A., Whitney, D.L., and Baharifar, A.A. (2004) Petrogenesis of andalusite-kyanite-sillimanite veins and host rocks, Sanandaj-Sirjan metamorphic belt, Hamadan, Iran. Journal of Metamorphic Geology, 22, 119–134.

Shaw, D.M. (1956) Geochemistry of pelitic rocks. Part III: Major elements and general geochemistry. Geological Society of America Bulletin, 67, 919–934.

Silliman, B. (1820) Sketches of a tour in the counties of New-Haven and Litchfield in Connecticut, with notices of the geology, mineralogy and scenery, &c. American Journal of Science, 2, 201–235.

Snow, D.T. (1969) Anisotropic permeability of fractured media. Water Resources Research, 5, 1273–1289.

Sorensen, S.S. and Grossman, J.N. (1989) Enrichment of trace elements in garnet-amphibolites from a paleo-subduction zone: Catalina Schist, Southern California. Geochimica et Cosmochimica Acta, 53, 3155–3177.

Spandler, C., Hermann, J., Arculus, R., and Mavrogenes, J. (2004) Geochemical heterogeneity and element mobility in deeply subducted oceanic crust; insights from high-pressure mafic rocks from New Caledonia. Chemical Geology, 206, 21–42.

Spiegel, M.R. (1961) Theory and problems of statistics, 359 p. McGraw-Hill, London.

Spiegelman, M. and Kelemen, P.B. (2003) Extreme chemical variability as a consequence of channelized melt transport. Geochemistry, Geophysics, Geosystems, 4(7), 1055, doi:10.1029/2002GC000336.

Teng, F., McDonough, W.F., Rudnick, R.L., and Wing, B.A. (2007) Limited lithium isotopic fractionation during progressive metamorphic dehydration in metapelites: A case study from the Onawa contact aureole, Maine. Chemical Geology, 239, 1–12.

Tracy, R.J., Rye, D.M., Hewitt, D.A., and Schiffries, C.M. (1983) Petrologic and stable-isotopic studies of fluid-rock interactions, south-central Connecticut: I. The role of infiltration in producing reaction assemblages in impure marbles. American Journal of Science, 283-A, 589–616.

Valley, J.M. and Kita, N.T. (2009) *In situ* oxygen isotope geochemistry by ion microprobe. In M. Fayek, Ed., Secondary ion mass spectrometry in the Earth sciences: Gleaning the big picture from a small spot, p. 19–63. Mineralogical Association of Canada, Short Course Series Volume 41.

van Haren, J.L.M., Ague, J.J., and Rye, D.M. (1996) Oxygen isotope record of fluid infiltration and mass transfer during regional metamorphism of pelitic schist, south-central Connecticut, USA. Geochimica et Cosmochimica Acta, 60, 3487–3504.

Walther, J.V. and Holdaway, M.J. (1995) Mass transfer during Barrovian Metamorphism of Pelites, south-central Connecticut—Comment. American Journal of Science, 295, 1020–1025.

Wohlers, A. and Manning, C.E. (2007) Model crustal fluids at high P and T: implications for Al transport. Geochimica et Cosmochimica Acta, 71, A1123.

——— (2009) Solubility of corundum in aqueous KOH solutions at 700 °C and 1 GPa. Chemical Geology, 262, 310–317.

Woronow, A. and Love, K.M. (1990) Quantifying and testing differences among means of compositional data suites. Mathematical Geology, 22, 837–852.

Wunder, B., Meixner, A., Romer, R.L., Feenstra, A., Schettler, G., and Heinrich, W. (2007) Lithium isotope fractionation between Li-bearing staurolite, Li-mica and aqueous fluids: An experimental study. Chemical Geology, 238, 277–290.

Yardley, B.W.D. (1975) On some quartz-plagioclase veins in the Connemara Schists, Ireland. Geological Magazine, 112, 183–190.

——— (1986) Fluid migration and veining in the Connemara Schists, Ireland. In J.V. Walther and B.J. Wood, Eds., Fluid-rock Interactions During Metamorphism, p. 107–131. Springer-Verlag, New York.

——— (2009) On the role of water in the evolution of the continental crust. Journal of the Geological Society, London, 166, 585–600.